Hindawi
Journal of Mathematics
Volume 2023, Article ID 6643772, 28 pages
https://doi.org/10.1155/2023/6643772

Research Article

Examining Dynamics of Emerging Nipah Viral Infection with Direct and Indirect Transmission Patterns: A Simulation-Based Analysis via Fractional and Fractal-Fractional Derivatives

Shuo Li,[1] Saif Ullah,[2] Salman A. AlQahtani,[3] and Joshua Kiddy K. Asamoah[4]

[1]*School of Mathematics and Data Sciences, Changji University, Changji, Xinjiang 831100, China*
[2]*Department of Mathematics, University of Peshawar, Peshawar, Pakistan*
[3]*Department of Information Systems, College of Computer and Information Sciences, King Saud University, P.O. Box 51178, Riyadh 11543, Saudi Arabia*
[4]*Department of Mathematics, Kwame Nkrumah University of Science and Technology, Kumasi, Ghana*

Correspondence should be addressed to Joshua Kiddy K. Asamoah; jkkasamoah@knust.edu.gh

Received 2 May 2023; Revised 2 August 2023; Accepted 7 September 2023; Published 6 October 2023

Academic Editor: Yusuf Gurefe

In this study, we examine the transmission dynamics of global Nipah virus infection under direct (human-to-human) and indirect (contaminated foods-to-human) transmission routes via the Caputo fractional and fractional-fractal modeling approaches. The model is vigorously analyzed both theoretically and numerically. The possible equilibrium points of the system and their existence are investigated based on the reproduction number. The model exhibits three equilibrium points, namely, infection-free, infected flying foxes free, and endemic. Furthermore, novel numerical schemes are derived for the models in fractional and fractal-fractional cases. Finally, an extensive simulation is conducted to validate the theoretical results and provide an impact of the model on the disease incidence. We believe that this study will help to incorporate such mathematical techniques to examine the complex dynamics and control the spread of such infectious diseases.

1. Introduction

1.1. Epidemiology of Nipah Virus. Nipah virus (NiV) is a zoonotic viral infection that was first reported in 1998 during an outbreak of encephalitis (inflammation of the brain) in Malaysia and Singapore. It was named after the village in Malaysia where the first outbreak occurred. The virus is mainly transmitted to humans from animals, particularly fruit bats (known as flying foxes), pigs, and other some domestic animals. The transmissions from human-to-human can also occur through direct contact with bodily fluids, such as blood, saliva, or respiratory secretions of infected individuals. The clinical symptoms of NiV infection can range from mild to severe and include headache, fever, muscle pain, vomiting, and respiratory illness. In severe cases, the infection can lead to encephalitis, seizures, and even coma with a higher risk of death. Still, there is no particular treatment for Nipah virus infection, and the best approach is supportive care to manage symptoms. Preventive measures include avoiding contact with infectious animals or their products and adopting good hygiene protocols, such as washing hands regularly and properly cooking meat. NiV outbreaks have occurred in numerous countries, including India, Bangladesh, and Malaysia, and have resulted in considerable public health and economic impacts. The virus is considered another potential pandemic threat due to its ability to cause severe illness and the lack of an effective treatment or vaccination [1, 2].

1.2. Literature Review. The mathematical modeling approach has been used substantially in epidemiology to better understand the transient and dynamics of infectious diseases, including NiV infection. These models are helpful for

researchers and health officials in setting the optimal interventions for controlling and preventing the spread of the disease. Numerous models can be used depending on the nature of the disease and the available dataset. For instance, ordinary differential equation (ODE) models are commonly used to study the dynamical aspects of infectious diseases in a homogeneously mixed population [3–5], while partial differential equation (PDE) models are suitable to analyze the spatial heterogeneity in disease spread [6–8]. On the other hand, stochastic models can incorporate randomness in disease transmission and help capture the effects of small populations and rare events [9, 10]. Recently, compartmental models with fractional-order differential equations have gained attention in the field of deadly contagious disease modeling. These fractional models are the generalization of the classical ODE models and account for noninteger-order derivatives, which can better capture complex dynamics and long-term memory effects to study the different epidemiological aspects of communicable diseases [11–15]. A novel study pertaining to the fractional fuzzy biological model has been developed in [16]. Fractional calculus, which involves operators of fractional order, has been increasingly used in recent years to model the complex biological and epidemiology phenomena due to its ability to capture memory and hereditary properties that are often found in these systems.

The Caputo operator, introduced by Michel Caputo in 1967, is one of the most commonly used fractional operators in modeling biological and epidemiological systems. The Caputo operator is a modified form of the Riemann–Liouville operator, and it has the advantage of being a local operator, which makes it computationally efficient [17]. Other famous operators with fractional order are the Caputo–Fabrizio (CF) [18] and the Atangana–Baleanu–Caputo (ABC) operators [19]. Moreover, in 2017, Atangana [20] introduced a new fractal-fractional operator which opens a new door to the modeling and understanding of the more complex problems including infections and diseases with crossover behavior. The well-developed fractional calculus and the fractal theory are combined to derive the new operators. The use of compartmental models with fractional-fractal operators to study the dynamics of various phenomena such as competition in commercial and rural banks and the recent COVID-19 pandemic were presented [21–23]. In [24], the authors successfully applied this new idea to explore the dynamical behavior of the monkeypox. Many compartmental models have been formulated and analyzed to explore the NiV infection dynamics. The dynamics and possible control of NiV infection outbreak in Bangladesh have been studied in [25]. A mathematical analysis via a compartmental model addressing the effective control intervention of this infection is being developed and analyzed in [26]. Recently, a number of NiV infection models with fractional derivatives with singular as well as nonsingular kernels have been presented in the literature (for instance, see [27–31]).

In most of the literature, NiV infection models are developed with the human-to-human transmission mode. In this study, we develop a compartmental epidemic model for the dynamics of NiV disease with food-born as well as human-to-human transmission from infected humans. Moreover, unlike the published literature, the model is constructed via fractional and fractional-fractal derivatives to gain valuable insights into the phenomena. The major sections covered in this study are as follows. The necessary definitions and results relevant to the study are recalled in Section 2. Model construction via the integer system is presented in detail in Section 3. The fractional extension of the problem with the basic mathematical analysis is studied in Section 4. Numerical treatment, i.e., derivation of the scheme and simulation are illustrated in Section 5. The extension of the NiV epidemic model in the FF operator perspective is presented in Section 6. In addition, this section covers the basic results, iterative scheme, and simulations of the NiV epidemic model in the FF case. The conclusion of the study is accomplished in Section 7.

2. Basic Fractional and Fractal-Fractional Theory

Fractional and FF differential operators have proven to play an essential role in mathematical modeling in various fields such as science, engineering, and epidemiology. In this section, we present necessary definitions that will be consistently utilized in this study [17, 20].

Definition 1. The Caputo derivative of $\Psi \in C^n[t_0, T]$ with t_0 is an initial time and is described by the following formula:

$$
\begin{aligned}
{}^{c}_{t_0}D^{\eta}_{t}\Psi(t) &= \left({}_{t_0}D^{-(m-\eta)}_{t}\left(\frac{d}{\mathrm{d}t}\right)^{m}\Psi(t)\right) = \frac{1}{\Gamma(m-\eta)}\int_{t_0}^{t}\Big((t-X)^{m-\eta-1}\Psi^{m}(X)\Big)\mathrm{d}X,\\
{}^{c}_{t}D^{\eta}_{t}\Psi(t) &= \left({}_{t}D^{-(m-\eta)}_{T}\left(-\frac{d}{\mathrm{d}t}\right)^{m}\Psi(t)\right) = \frac{(-1)^{m}}{\Gamma(m-\eta)}\int_{t}^{T}\Big((X-t)^{m-\eta-1}\Psi^{m}(X)\Big)\mathrm{d}X.
\end{aligned}
\tag{1}
$$

Definition 2. For $r \in \mathbb{R}$, the Mittag–Leffler function in a generalized form of $E_{\alpha,\beta}(r)$ is defined by

$$E_{\alpha,\beta}(r) = \sum_{m=0}^{\infty} \frac{x^m}{\Gamma(\alpha m + \beta)}, \quad \alpha > 0, \beta > 0, \tag{2}$$

such that

$$E_{\alpha,\beta}(r) = rE_{\alpha,\alpha+\beta}(r) + \frac{1}{\Gamma(\beta)}. \tag{3}$$

We define the Laplace of $t^{\beta-1}E_{\alpha,\beta}(\pm\lambda t^{\alpha})$ by using the following equation:

$$L\left[t^{\beta-1}E_{\alpha,\beta}\left(\pm\lambda t^{\alpha}\right)\right] = \frac{s^{\alpha-\beta}}{s^{\alpha} \mp \lambda}. \tag{4}$$

Definition 3. The equilibrium point of a system described via the Caputo-type derivative is

$${}^{C}D_t^{\eta} y(t) = F(t, y(t)), \quad \eta \in (0,1), \tag{5}$$

where the point $y = y^*$ if and only if $F(t, y^*) = 0$. Let Ψ be the continuously fractal differentiable function of (a_1, a_2). Then, the fractional and fractal dimensions are η and ϑ.

Definition 4. The FF operator based on power law is stated as [20]

$${}^{FF-P}D_{0,t}^{\eta,\vartheta}(\Psi) = \frac{1}{\Gamma(n-\eta)} \frac{d}{dt^{\vartheta}} \int_0^t (t-\zeta)^{n-\eta-1}\Psi(\zeta)\mathrm{d}\zeta, \tag{6}$$

where $\eta, \vartheta \in (n-1, n]$ and $n \in \mathbb{N}$ and $d\Psi(\xi)/\mathrm{d}\xi^{\vartheta} = \lim_{t \longrightarrow \xi} \Psi - \Psi(\xi)/t^{\vartheta} - \xi^{\vartheta}$.

Definition 5. The integral for the FF operator (6) is stated as follows:

$${}^{FF-P}J_{0,t}^{\eta}(\Psi(t)) = \frac{\vartheta}{\Gamma(\eta)} \int_0^t (t-\zeta)^{\eta-1}\zeta^{\vartheta-1}\Psi(\zeta)\mathrm{d}\zeta. \tag{7}$$

3. Formulating Dynamics of the NiV Infection in Integer Case

This section briefly covers the construction criteria of the transmission model addressing the dynamical aspects of NiV disease in the integer case. The model includes two modes of transmission. The food-borne transmission is when the virus transmits through contaminated food and the direct person-to-person transmission from both deceased and infected humans. The model consists of seven differential equations that describe the dynamic aspects of different populations. The virus shedding by infected flying at time t for foxes is denoted by $V(t)$. The population of flying foxes is divided into two subgroups: susceptible flying foxes denoted by S_f and infected flying foxes denoted by I_f. The infected flying foxes I_f transmit the virus to the human population. The flying foxes are believed to be the natural hosts of the NiV virus.

The human population is subdivided into four subgroups: susceptible S, infectious I, recovered R, and deceased D humans, respectively. The details of each case are as follows:

(i) S: the susceptible human population that has not been infected with NiV

(ii) I: the infected human population that is currently infected with NiV

(iii) H: the hospitalized or under treatment infected individuals

(iv) R: the recovered human population that has recovered from NiV and has developed immunity against it

(v) D: the deceased human population that has succumbed due to NiV infection

3.1. Virus Dynamics. The symbol p indicates the rate at which the virus is generated via the infected flying foxes. θ is the rate at which the virus decays over time. The viruses' compartment dynamics is, therefore, modeled by the following equation:

$$\frac{dV(t)}{\mathrm{d}t} = pI_f - \theta V. \tag{8}$$

3.2. Submodel of Flying Foxes. The parameter Λ_f is the respective recruitment rate of S_f and μ_f is the natural death rate. The suspectable flying foxes' population gained infection at the rate β_1 where the force of infection is shown by $\beta_1 VS_f/N_f$. The infected flying foxes are enhanced by joining the susceptible flying foxes after getting infected and die at the rate of μ_f. Thus, the following subsystem is obtained for the dynamics of the flying foxes population:

$$\begin{aligned} \frac{dS_f(t)}{\mathrm{d}t} &= \Lambda_f - \frac{\beta_1 VS_f}{N_f} - \mu_f S_f, \\ \frac{dI_f(t)}{\mathrm{d}t} &= \frac{\beta_1 VS_f}{N_f} - \mu_f I_f. \end{aligned} \tag{9}$$

3.3. Submodel of Human Population. The population in the susceptible human class is recruited by Λ_h and reduced at the natural mortality of μ_h. The susceptible humans acquire infection through indirect transmission routes at the rate of β_2. These human populations further become infected as a result of contracting infections from individuals and dead bodies (those with the Nipah virus) at a rate of β_3 and β_4, respectively. The term used for describing the infection force for the human population case is given by

$$\lambda_h = \frac{\beta_2 V + \kappa\beta_3 D + \beta_4 I}{N_h}. \tag{10}$$

The parameter κ indicates a fraction of those deceased humans not properly handled. The infectious human class is increased by joining susceptible individuals with the force of infection λ_h. This population has a decreased recovery rate α_1

with decreased disease-related and natural mortality rates and μ_h, respectively. The infected people joined hospitalized (or under treatment) classes at the rate of ρ. The hospitalized human class is enhanced by hospitalizing the infectious people at the rate of ρ. These populations move to the recovered class after proper treatment at the rate of σ. The hospitalized population is further decreased due to natural and disease-induced death rates denoted by μ_h and μ_1, respectively. The recovered class is enhanced by joining the infectious and hospitalized individuals after acquiring immunity and becoming susceptible due to loss of immunity at the rate of γ. This is further decreased due to the natural death rate μ_h. Finally, the class of deceased humans is increased due to the Nipah-induced and natural mortality rates and μ_h, respectively. This class is reduced at the rate of dead bodies obliteration ν. Thus, the following system is obtained for the dynamics of the human population:

$$\begin{aligned}
\frac{dS(t)}{dt} &= \Lambda_h - \frac{(\beta_2 V + \beta_3 \kappa D + \beta_4 I)S}{N_h} - \mu_h S + \gamma R,\\
\frac{dI(t)}{dt} &= \frac{(\beta_2 V + \beta_3 \kappa D + \beta_4 I)S}{N_h} - (\alpha_1 + \alpha_2 + \rho + \mu_h)I,\\
\frac{dH(t)}{dt} &= \rho I - (\sigma + \mu_1 + \mu_h)H,\\
\frac{dR(t)}{dt} &= \alpha_1 I + \sigma H - (\gamma + \mu_h)R,\\
\frac{dD(t)}{dt} &= (\alpha_2 + \mu_h)I - \nu D.
\end{aligned} \tag{11}$$

By combining (8) to (11), we construct the following model consisting of seven differential equations and describe the dynamics of NiV infection:

$$\begin{aligned}
\frac{dV(t)}{dt} &= pI_f - \theta V,\\
\frac{dS_f(t)}{dt} &= \Lambda_f - \frac{\beta_1 V S_f}{N_f} - \mu_f S_f,\\
\frac{dI_f(t)}{dt} &= \frac{\beta_1 V S_f}{N_f} - \mu_f I_f,\\
\frac{dS(t)}{dt} &= \Lambda_h - \frac{(\beta_2 V + \kappa\beta_3 D + \beta_4 I)S}{N_h} - \mu_h S + \gamma R,\\
\frac{dI(t)}{dt} &= \frac{(\beta_2 V + \kappa\beta_3 D + \beta_4 I)S}{N_h} - (\alpha_1 + \alpha_2 + \rho + \mu_h)I,\\
\frac{dH(t)}{dt} &= \rho I - (\sigma + \mu_1 + \mu_h)H,\\
\frac{dR(t)}{dt} &= \alpha_1 I + \sigma H - (\gamma + \mu_h)R,\\
\frac{dD(t)}{dt} &= (\alpha_2 + \mu_h)I - \nu D,
\end{aligned} \tag{12}$$

with respective nonnegative initial conditions (ICs) as

$$\left.\begin{aligned}
V(0) = V_0 \geq 0, S_f(0) = S_{f_0} \geq 0, I_f(0) = I_{f_0} \geq 0, S(0) = S_0 \geq 0\\
I(0) = I_0 \geq 0, H(0) = H_0 \geq 0, R(0) = R_0 \geq 0, \text{and } D(0) = D_0 \geq 0
\end{aligned}\right\}. \tag{13}$$

4. NiV Dynamics via Fractional Derivative

Using fractional derivatives in modeling can be a powerful tool for understanding complex biological systems that exhibit memory and hereditary effects. In many real-life situations including biological problems, the virus behavior only at the initial point for $t = 0$ is not sufficient to reflect the dynamics of the virus at $t = t_1$. For this reason, it is necessary that all past behavior from 0 to t_1 must be considered. The inclusion of fractional derivatives is essential to capture the hereditary as well as the memory effects required for such a scenario. Consequently, the integer derivative of the NiV model (12) is substituted with a derivative of a noninteger order. The Caputo-type of fractional derivative commonly used in mathematical modeling is considered in this study. The subsequent NiV fractional epidemic model is summarized in the following system:

$$\begin{cases} \dfrac{dV}{dt} = \displaystyle\int_{t_0}^{t} \mathscr{K}\left(t-t'\right)\left[pI_f - \theta V\right]dt', \\ \dfrac{dS_f}{dt} = \displaystyle\int_{t_0}^{t} K\left(t-t'\right)\left[\Lambda_f - \dfrac{\beta_1 S_f V}{N_f} - \mu_f S_f\right]dt', \\ \dfrac{dI_f}{dt} = \displaystyle\int_{t_0}^{t} \mathscr{K}\left(t-t'\right)\left[\dfrac{\beta_1 S_f V}{N_f} - \mu_f I_f\right]dt', \\ \dfrac{dS}{dt} = \displaystyle\int_{t_0}^{t} \mathscr{K}\left(t-t'\right)\left[\Lambda_h - \dfrac{(\beta_2 V + \kappa\beta_3 D + \beta_4 I)S}{N_h} - \mu_h S + \gamma R\right]dt', \\ \dfrac{dI}{dt} = \displaystyle\int_{t_0}^{t} \mathscr{K}\left(t-t'\right)\left[\dfrac{(\beta_2 V + \kappa\beta_3 D + \beta_4 I)S}{N_h} - (\alpha_1 + \alpha_2 + \rho + \mu_h)I\right]dt', \\ \dfrac{dH}{dt} = \displaystyle\int_{t_0}^{t} \mathscr{K}\left(t-t'\right)\left[\rho I - (\sigma + \mu_1 + \mu_h)H\right]dt', \\ \dfrac{dR}{dt} = \displaystyle\int_{t_0}^{t} \mathscr{K}\left(t-t'\right)\left[\alpha_1 I + \sigma H - (\gamma + \mu_h)R\right]dt', \\ \dfrac{dD}{dt} = \displaystyle\int_{t_0}^{t} \mathscr{K}\left(t-t'\right)\left[(\alpha_2 + \mu_h)I - \nu D\right]dt'. \end{cases} \tag{14}$$

The expression $\mathscr{K}(t-t')$ in (14) illustrates that the respective kernel depends on time such that

$$\mathscr{K}\left(t-t'\right) = \frac{\left(t-t'\right)^{\eta-2}}{\Gamma(\eta-1)}. \tag{15}$$

By introducing (15) in (14) and by making use of the Caputo derivative of order $\eta - 1$, we get

$$\begin{cases} {}^{C}D_t^{\eta-1}\left[\dfrac{dV}{dt}\right] = {}^{C}D_t^{\eta-1} I_t^{-(\eta-1)}\left[pI_f - \theta V\right], \\ {}^{C}D_t^{\eta-1}\left[\dfrac{dS_f}{dt}\right] = {}^{C}D_t^{\eta-1} I_t^{-(\eta-1)}\left[\Lambda_f - \dfrac{\beta_1 S_f V}{N_f} - \mu_f S_f\right], \\ {}^{C}D_t^{\eta-1}\left[\dfrac{dI_f}{dt}\right] = {}^{C}D_t^{\eta-1} I_t^{-(\eta-1)}\left[\dfrac{\beta_1 S_f V}{N_f} - \mu_f I_f\right], \\ {}^{C}D_t^{\eta-1}\left[\dfrac{dS}{dt}\right] = {}^{C}D_t^{\eta-1} I_t^{-(\eta-1)}\left[\Lambda_h - \dfrac{(\beta_2 V + \kappa\beta_3 D + \beta_4 I)S}{N_h} - \mu_h S + \gamma R\right], \\ {}^{C}D_t^{\eta-1}\left[\dfrac{dI}{dt}\right] = {}^{C}D_t^{\eta-1} I_t^{-(\eta-1)}\left[\dfrac{(\beta_2 V + \kappa\beta_3 D + \beta_4 I)S}{N_h} - (\alpha_1 + \alpha_2 + \rho + \mu_h)I\right], \\ {}^{C}D_t^{\eta-1}\left[\dfrac{dH}{dt}\right] = {}^{C}D_t^{\eta-1} I_t^{-(\eta-1)}\left[\rho I - (\sigma + \mu_1 + \mu_h)H\right], \\ {}^{C}D_t^{\eta-1}\left[\dfrac{dR}{dt}\right] = {}^{C}D_t^{\eta-1} I_t^{-(\eta-1)}\left[\alpha_1 I + \sigma H - (\gamma + \mu_h)R\right], \\ {}^{C}D_t^{\eta-1}\left[\dfrac{dD}{dt}\right] = {}^{C}D_t^{\eta-1} I_t^{-(\eta-1)}\left[(\alpha_2 + \mu_h)I - \nu D\right]. \end{cases} \tag{16}$$

The fractional NiV epidemic model leads to the following form after some simplifications:

$$
\begin{aligned}
{}^{C}D_t^{\eta}V &= pI_f - \theta V,\\
{}^{C}D_t^{\eta}S_f &= \Lambda_f - \frac{\beta_1 S_f V}{N_f} - \mu_f S_f,\\
{}^{C}D_t^{\eta}I_f &= \frac{\beta_1 S_f V}{N_f} - \mu_f I_f,\\
{}^{C}D_t^{\eta}S &= \Lambda_h - \frac{(\beta_2 V + \kappa\beta_3 D + \beta_4 I)S}{N_h} - \mu_h S + \gamma R,\\
{}^{C}D_t^{\eta}I &= \frac{(\beta_2 V + \kappa\beta_3 D + \beta_4 I)S}{N_h} - q_1 I,\\
{}^{C}D_t^{\eta}H &= \rho I - q_2 H,\\
{}^{C}D_t^{\eta}R &= \alpha_1 I + \sigma H - q_3 R,\\
{}^{C}D_t^{\eta}D &= q_4 I - \nu D,
\end{aligned}
\tag{17}
$$

where $q_1 = (\alpha_1 + \alpha_2 + \rho + \mu_h), q_2 = (\sigma + \mu_1 + \mu_h), q_3 = (\gamma + \mu_h)$, and $q_4 = (\alpha_2 + \mu_h)$.

With subject to the nonnegative conditions in (13), in system (17), $q_1 = (\alpha_1 + \alpha_2 + \rho + \mu_h), q_2 = (\sigma + \mu_1 + \mu_h), q_3 = (\gamma + \mu_h)$, and $q_4 = (\alpha_2 + \mu_h)$ are the derivatives of Caputo sense where $\eta \in (0, 1]$.

4.1. Basic Properties of the NiV Epidemic Fractional Model. The primary aim of this section is to provide some of the necessary mathematical features of the NiV epidemic model developed in (17).

4.1.1. Invariant Region and Boundedness

Theorem 6. *The model in (17) with ICs stated in (12) has an invariantly positive solution in* $\Xi = \Xi_f \times \Xi_h$, *where*

$$
\begin{aligned}
\Xi_f &= \left\{\left(V, S_f, I_f\right) \in \mathbb{R}_+^3, \text{and } N_f = \left(S_f + I_f\right) \le \frac{\Lambda_f}{\mu_f}, V \le \frac{p\Lambda_f}{\theta\mu_f}\right\},\\
\Xi_h &= \left\{(S, I, H, R, D) \in \mathbb{R}_+^5, \text{and } N_h = (S + I + H + R) \le \frac{\Lambda_h}{\mu_h}, D \le \frac{\Lambda_h(\alpha_2 + \mu_h)}{\nu\mu_h}\right\}.
\end{aligned}
\tag{18}
$$

Proof. We proceed with the proof of the abovementioned theorem. Initially, by adding the equations of only flying foxes population in model (17), we get

$$
\begin{aligned}
{}^{C}D_t^{\eta}N_f &= {}^{C}D_t^{\eta}S_f + {}^{C}D_t^{\eta}I_f\\
&= \Lambda_f - \mu_f N_f,
\end{aligned}
\tag{19}
$$

or

$${}^{C}D_t^{\eta}N_f + \mu_f N_f = \Lambda_f. \tag{20}$$

By taking the Laplace transform on both sides, we get

$$
\begin{aligned}
\mathscr{L}\left[{}^{C}D_t^{\eta}N_f + \mu_f N_f\right] &= \mathscr{L}\left[\Lambda_f\right],\\
s^{\eta}N_f(s) - s^{\eta-1}N_f(0) + \mu_f N_f(s) &= \frac{\Lambda_f}{s},\\
\left(s^{\eta} + \mu_f\right)N_f(s) &= \frac{\Lambda_f}{s} + s^{\eta-1}N_f(0),\\
N_f(s) &= \frac{\Lambda_f}{s\left(s^{\eta} + \mu_f\right)} + \frac{s^{\eta-1}N_f(0)}{\left(s^{\eta} + \mu_f\right)}.
\end{aligned}
\tag{21}
$$

By applying the inverse Laplace transform and after some adstipulation, we obtain

$$N_f(t) \le \frac{\Lambda_f}{\mu_f} + \left(N_f(0) - \frac{\Lambda_f}{\mu_f}\right)\mathscr{E}_{\eta}\left(-\mu_f t^{\eta}\right), \tag{22}$$

where $\mathscr{E}_{\eta}(-\mu_f t^{\eta})$ is the Mittag–Leffler function of parameter η. Clearly, if $N_f(0) \le \Lambda_f/\mu_f$, then $N_f(t) \le \Lambda_f/\mu_f$ as $t \longrightarrow \infty$.

So, $N_f(t)$ converges as $t \longrightarrow \infty$. Moreover, for $t > 0$, the model solution with IC in Ξ_f remains in Ξ_f.

Furthermore, we consider the first equation denoting the dynamics of virus concentration and keeping in mind that $F_I \le \Lambda_f/\mu_f$. Thus, we have

$$
\begin{aligned}
{}^{C}D_t^{\eta}V(t) + \theta V &\le \frac{p\Lambda_f}{\mu_f},\\
\mathscr{L}\left[{}^{C}D_t^{\eta}V(t) + \theta V\right] &\le \mathscr{L}\left[\frac{p\Lambda_f}{\mu_f}\right],\\
V(s) &\le \frac{p\Lambda_f}{\mu_f s\left(s^{\eta} + \theta\right)} + \frac{s^{\eta-1}V(0)}{\left(s^{\eta} + \theta\right)}.
\end{aligned}
\tag{23}
$$

In a similar way, by applying the inverse Laplace transform and after some adstipulation, we obtain that

$$V(t) \leq \frac{p\Lambda_f}{\theta\mu_f} + \left(V(0) - \frac{p\Lambda_f}{\theta\mu_f}\right)\mathscr{E}_\eta\left(-\theta t^\eta\right). \tag{24}$$

Thus, if $(0) \leq \Lambda_f/\mu_f$, then $V(t) \leq p\Lambda_f/\theta\mu_f$, as $t \longrightarrow \infty$. By following a similar approach, in the case of human subcompartments, we obtain

$$N_h(t) \leq \frac{\Lambda_h}{\mu_h} + \left(N_h(0) - \frac{\Lambda_h}{\mu_h}\right)\mathscr{E}_\eta\left(-\mu_h t^\eta\right),$$

$$\text{and } D(t) \leq \frac{(\mu_h + \alpha_2)}{\nu}\frac{\Lambda_h}{\mu_h} + \left(D(0) - \frac{(\mu_h + \alpha_2)}{\nu}\frac{\Lambda_h}{\mu_h}\right)\mathscr{E}_\eta\left(-\nu t^\eta\right). \tag{25}$$

Hence, if $N_h(0) \leq \Lambda_h/\mu_h$ and $D(0) \leq (\mu_h + \alpha_2)/\nu\Lambda_h/\mu_h$, then $N_h(t) \leq \Lambda_h/\mu_h$ and $D(t) \leq (\mu_h + \alpha_2)/\nu\Lambda_h/\mu_h$ as $t \geq 0$ and $t \longrightarrow \infty$. Thus, the set Ξ is positively invariant for the NiV model (17) and attract all the solutions of the system in Ξ. □

4.1.2. Existence and Uniqueness of the Problem Solution. In this section, we aim to prove the problem solution's existence and positivity. The well-known mean value theorem from [32] is employed for the said purpose. The following theorem is recalled to proceed with the desired proof.

Lemma 7 (see [32]). *Let $\mathscr{F}(t) \in C[m_1, m_2]$ and $\mathscr{F}(t){}^{C}_{m_1}D^{\eta}_{t} \in C(m_1, m_2]$, then we have*

$$\mathscr{F}(t) = \mathscr{F}(m_1) + \frac{1}{\Gamma(\eta)}\left({}^{C}_{m_1}D^{\eta}_{t}\mathscr{F}\right)(\zeta)(t - m_1)^\eta, \tag{26}$$

such that $m_1 \leq \zeta \leq t$ and $\forall t \in (m_1, m_2]$.

Corollary 8 (see [32]). *Let $\mathscr{F}(t) \in C[m_1, m_2]$ and ${}^{C}_{m_1}D^{\eta}_{t}\mathscr{F}(t) \in C(m_1, m_2]$, where $\eta \in (0, 1]$, then if*

(i) ${}^{C}_{m_1}D^{\eta}_{t}\mathscr{F}(t) \geq 0, \forall t \in (m_1, m_2)$, then $\mathscr{F}(t)$ is nondecreasing

(ii) ${}^{C}_{m_1}D^{\eta}_{t}\mathscr{F}(t) \leq 0, \forall t \in (m_1, m_2)$, then $\mathscr{F}(t)$ is nonincreasing

The theorem that follows provides the proof of the aforementioned results.

Theorem 9. *The NiV epidemic model in fractional case (17) has a unique and nonnegative solution.*

Proof. To prove the fundamental properties of the model solution, we follow the facts provided in [33]. It is easy to confirm the existence of the solution by using the mentioned literature. Furthermore, by using Remark 3.2 in [33], the solution's uniqueness can be shown. Finally, to prove the solution's nonnegativity, it is necessary that over each hyperplane with bounding positive orthant, the vector field points to $\mathbb{R}^8_+$. From the NiV epidemic model (17), we proceed as

$$\begin{aligned}
{}^{C}D^{\eta}_{t}V(t)\big|_{V=0} &= pI_f \geq 0,\\
{}^{C}D^{\eta}_{t}S_f(t)\big|_{S_f=0} &= \Lambda_f \geq 0,\\
{}^{C}D^{\eta}_{t}I_f(t)\big|_{I_f=0} &= \lambda_f S_f \geq 0,\\
{}^{C}D^{\eta}_{t}S(t)\big|_{S=0} &= \Lambda_h + \gamma R \geq 0,\\
{}^{C}D^{\eta}_{t}I(t)\big|_{I=0} &= \lambda_h S \geq 0,\\
{}^{C}D^{\eta}_{t}H(t)\big|_{H=0} &= \rho I \geq 0,\\
{}^{C}D^{\alpha}_{t}R(t)\big|_{R=0} &= \alpha_1 I + \sigma H \geq 0,\\
{}^{C}D^{\alpha}_{t}D(t)\big|_{D=0} &= q_3 I \geq 0.
\end{aligned} \tag{27}$$

Thus, following the results in the above cited literature, it proves that the entire solution will remain in $\mathbb{R}^8_+$, for all $t \geq 0$. □

4.1.3. Investigation of Equilibria and Threshold Parameter. This section provides an in-depth examination of the equilibrium states of the model and the conditions under which they exist. The NiV-free equilibrium point (NVFE) of system (17) is evaluated as

$$E^0 = \left(V^0, S_f^0, I_f^0, S^0, I^0, H^0, R^0, D^0\right) = \left(0, \frac{\Lambda_f}{\mu_f}, 0, \frac{\Lambda_h}{\mu_h}, 0, 0, 0, 0\right). \tag{28}$$

We compute the basic reproductive number $\mathscr{R}_0$ via the well-defined approach, and it can be expressed as

$$\begin{aligned}
\mathscr{R}_0 &= \max\left\{\mathscr{R}_f^0, \mathscr{R}_h^0\right\} = \max\left\{\mathscr{R}_f^0, \mathscr{R}_{h_1}^0 + \mathscr{R}_{h_2}^0\right\}\\
&= \max\left\{\frac{p\beta_1}{\theta\mu_f}, \frac{\beta_4}{q_1} + \frac{q_4\kappa\beta_3}{\nu q_1}\right\},
\end{aligned} \tag{29}$$

where

$$\begin{aligned}
\mathscr{R}_f^0 &= \frac{p\beta_1}{\theta\mu_f},\\
\mathscr{R}_{h_1}^0 &= \frac{\beta_4}{q_1},\\
\mathscr{R}_{h_2}^0 &= \frac{q_4\kappa\beta_3}{\nu q_1}.
\end{aligned} \tag{30}$$

4.1.4. Infected Flying Foxes Free Equilibrium State

Theorem 10. *For the NiV model (17), when $\mathscr{R}_0 > 1$, an infected flying foxes free equilibrium (IFFE) point exists, which is unique in nature.*

Proof. By solving equation (17) simultaneously in terms of virus and human compartments and by setting $S_f = \Lambda_f/\mu_f$,

$I_f = 0$, and $V = 0$, the resulting expression for the IFFE point is as follows:

$$E_h^{**} = \left(0, \frac{\Lambda_f}{\mu_f}, 0, S^{**}, I^{**}, H^{**}, R^{**}, D^{**}\right), \tag{31}$$

such that

$$\begin{cases} S^{**} = \dfrac{q_1q_2q_3\Lambda_H^{**}}{\{q_1q_2q_3 - (\gamma\rho\sigma + \alpha_1\gamma q_2)\}\lambda_h^{**} + q_1q_2q_3\mu_h}, \\ I^{**} = \dfrac{\lambda_h^{**}S^{**}}{q_1}, \\ H^{**} = \dfrac{\lambda_h^{**}S^{**}\rho}{q_1q_2}, \\ R^{**} = \dfrac{(\rho\sigma + \alpha_1 q_2)S^{**}\lambda_h^{**}}{q_1q_2q_3}, \\ D^{**} = \dfrac{S^{**}\lambda_h^{**}q_4}{\nu q_1}, \end{cases} \tag{32}$$

where

$$\lambda_h^{**} = \frac{\beta_2 V^{**} + \beta_4 I^{**} + \kappa\beta_3 D^{**}}{N_h^{**}}. \tag{33}$$

Furthermore, by putting (37) in (33), we obtain

$$b_1\lambda_h^{**} + b_2 = 0, \tag{34}$$

where the coefficients are

$$\begin{aligned} b_1 &= \nu\Lambda_h(\alpha_1 q_2 + q_3(q_2 + \rho) + \rho\sigma), \\ b_2 &= q_1q_2q_3\nu\Lambda_H\left(1 - \mathscr{R}_h^0\right). \end{aligned} \tag{35}$$

The term $\{q_1q_2q_3 - (\gamma\rho\sigma + \alpha_1\gamma q_2)\}$ is positive; therefore, a unique IFFE point exits when $\mathscr{R}_h^0 > 1$. It means that the disease is endemic in the human population when $\mathscr{R}_h^0 > 1$. □

4.1.5. NiV Endemic Equilibrium Point. By solving (17) simultaneously at a steady state in terms of λ_H^{**}, we get the NiV endemic equilibrium (NVEE) as

$$E^{**} = \left(V^{**}, S_f^{**}, I_f^{**}, S^{**}, I^{**}, H^{**}, R^{**}, D^{**}\right), \tag{36}$$

where

$$\begin{cases} V^{**} = \dfrac{p\beta_1\Lambda_f^{**} - \theta\Lambda_f^{**}\mu_f}{\theta\beta_1\mu_f}, \\ S_f^{**} = \dfrac{\theta\Lambda_f^{**}}{p\beta_1}, \\ I_f^{**} = \dfrac{\Lambda_f^{**}}{\mu_f} - \dfrac{\theta\Lambda_f^{**}}{p\beta_1}, \\ S^{**} = \dfrac{q_1q_2q_3\Lambda_H^{**}}{\{q_1q_2q_3 - (\gamma\rho\sigma + \alpha_1\gamma q_2)\}\lambda_h^{**} + q_1q_2q_3\mu_h}, \\ I^{**} = \dfrac{\lambda_h^{**}S^{**}}{q_1}, \\ H^{**} = \dfrac{\lambda_h^{**}S^{**}\rho}{q_1q_2}, \\ R^{**} = \dfrac{(\rho\sigma + \alpha_1 q_2)S^{**}\lambda_h^{**}}{q_1q_2q_3}, \\ D^{**} = \dfrac{S^{**}\lambda_h^{**}q_4}{\nu q_1}, \end{cases} \tag{37}$$

$$V^{**} = \frac{p\beta_1\Lambda_f^{**} - \theta\Lambda_f^{**}\mu_f}{\theta\beta_1\mu_f}, F_S^{**} = \frac{\theta\Lambda_f^{**}}{p\beta_1},$$

$$F_I^{**} = \frac{\Lambda_f^{**}}{\mu_f} - \frac{\theta\Lambda_f^{**}}{p\beta_1},$$

$$H_S^{**} = \frac{q_1q_2\Lambda_H^{**}}{q_1q_2\lambda_H^{**} - \gamma\alpha_1\lambda_H^{**} + q_1q_2\mu_h},$$

$$H_I^{**} = \frac{\lambda_H^{**}H_S^{**}}{q_1}, H_R^{**} = \frac{\alpha_1 H_I^{**}}{q_2},$$

$$H_D^{**} = \frac{q_3H_I^{**}}{\nu},$$

and λ_H^{**} as the solution of

$$b_0\lambda_H^{**2} + b_1\lambda_H^{**} + b_2 = 0, \tag{38}$$

where

$$\begin{aligned} b_2 &= \nu q_1 q_2 q_3\left(1 - R_f^0\right)\beta_2\Lambda_f\mu_h, \\ b_1 &= \nu\left(q_2\left(q_1q_3 - \gamma\alpha_1\right) - \gamma\rho\sigma\right)\beta_2\Lambda_f\left(1 - \mathscr{R}_f^0\right) \\ &\quad + \nu q_1 q_2 q_3\beta_1\Lambda_h\left(1 - \mathscr{R}_h^0\right), \\ b_0 &= \nu\Lambda_h\left(\alpha_1 q_2 + q_3\left(q_2 + \rho\right) + \rho\sigma\right). \end{aligned} \tag{39}$$

The following theorem regarding NVEE is developed.

Theorem 11

(i) A NVEE point E^{**} exists and will be unique if $b_2 < 0 \Leftrightarrow \mathscr{R}_f^0 \geq 1$

(ii) The point E^{**} will be unique if $(b_1 < 0 \wedge b_2 = 0) \vee b_1^2 - 4b_0b_2 = 0$

(iii) If $b_1 < 0, b_2 > 0$, and the discriminant is positive, then the model possesses two NVEE

(iv) No NVEE will exist elsewhere

In view of condition (i), a unique NVEE exists for the model.

5. Numerical Investigation of the Caputo NiV Model

This section accomplishes the iterative scheme of the NiV (17) in the Caputo sense. In addition to confirm the theoretical results, simulation will be performed in detail.

5.1. Iterative Scheme. The modified Euler's scheme in the fractional case is employed to establish the integrative scheme of the problem [34]. The method is simple and provides a reliable solution. To develop the desired solution, the fractional epidemic model (17) is comprehensively described as follows:

$$\begin{cases} {}^{C}D_t^{\eta} f(t) = \mathscr{G}(t, f(t)), \\ f(0) = f_0, \quad 0 < \mathscr{T} < \infty, \end{cases} \tag{40}$$

where $f(t) = (V, S_f, I_f, S, I, H, R, D) \in \mathbb{R}^8$. f_0 shows that the initial state vector corresponds to the problem under consideration. Furthermore, $\mathscr{G}(t, f(t)) = (\mathscr{G}_1(t, f(t)), \mathscr{G}_2(t, f(t)), \mathscr{G}_3(t, f(t)), \mathscr{G}_4(t, f(t)), \mathscr{G}_5(t, f(t)), \mathscr{G}_6(t, f(t)), \mathscr{G}_7(t, f(t)))$ is a real-valued continuous vector function that fulfils the well-known Lipschitz condition described as follows:

$$\begin{cases} \mathscr{G}_1(t, f(t)) = pI_f - \theta V, \\ \mathscr{G}_2(t, f(t)) = \Lambda_f - \dfrac{\beta_1 S_f V}{N_f} - \mu_f S_f, \\ \mathscr{G}_3(t, f(t)) = \dfrac{\beta_1 S_f V}{N_f} - \mu_f I_f, \\ \mathscr{G}_4(t, f(t)) = \Lambda_h - \dfrac{(\beta_2 V + \kappa\beta_3 D + \beta_4 I)S}{N_h} - \mu_h S + \gamma R, \\ \mathscr{G}_5(t, f(t)) = \dfrac{(\beta_2 V + \kappa\beta_3 D + \beta_4 I)S}{N_h} - q_1 I, \\ \mathscr{G}_6(t, f(t)) = \rho I - q_2 H, \\ \mathscr{G}_7(t, f(t)) = \alpha_1 I + \sigma H - q_3 R, \\ \mathscr{G}_8(t, f(t)) = q_4 I - \nu D. \end{cases} \tag{41}$$

By taking integral in the Caputo sense over both sides of (40), it is simplified as

$$f(t) = f_0 + \frac{1}{\Gamma(\eta)}\int_0^t (t - \varsigma)^{\eta-1}\mathscr{G}(\varsigma, f(\varsigma))\mathrm{d}\varsigma. \tag{42}$$

To proceed, let us consider a uniform grid over $[0, \mathscr{T}]$, having a step size of $\mathfrak{h} = \mathscr{T} - 0/m$, where $m \in \mathbb{N}$. The application of a well-known Euler method in fractional cases [34] leads to problem (42) as

$$\begin{cases} f_{n+1} = f_0 + \dfrac{\mathfrak{h}^{\eta}}{\Gamma(\eta + 1)}\displaystyle\sum_{\iota=0}^{n}\left((n - \iota + 1)^{\eta} - (n - \iota)^{\eta}\right)\mathscr{G}\left(t_\iota, f\left(t_\iota\right)\right), \quad n = 0, \ldots, m. \end{cases} \tag{43}$$

Thus, by using the scheme derived in (43), the iterative formulae for the proposed NiV fractional case model (17) are obtained as

$$
\begin{aligned}
V_{n+1} &= V_0 + \frac{\mathfrak{h}^{\eta}}{\Gamma(\eta+1)}\sum_{\iota=0}^{n}\left((n+1-\iota)^{\eta}-(n-\iota)^{\eta}\right)\left(pI_{f\iota}-\theta V_{\iota}\right),\\
S_{fn+1} &= S_{f0} + \frac{\mathfrak{h}^{\eta}}{\Gamma(\eta+1)}\sum_{\iota=0}^{n}\left((n+1-\iota)^{\eta}-(n-\iota)^{\eta}\right)\left(\Lambda_f - \frac{\beta_1 S_{f\iota} V_{\iota}}{N_{f\iota}} - \mu_f S_{f\iota}\right),\\
I_{fn+1} &= I_{f0} + \frac{\mathfrak{h}^{\eta}}{\Gamma(\eta+1)}\sum_{\iota=0}^{n}\left((n+1-\iota)^{\eta}-(n-\iota)^{\eta}\right)\left(\frac{\beta_1 S_{f\iota} V_{\iota}}{N_{f\iota}} - \mu_f I_{f\iota}\right),\\
S_{n+1} &= S_0 + \frac{\mathfrak{h}^{\eta}}{\Gamma(\eta+1)}\sum_{\iota=0}^{n}\left((n+1-\iota)^{\eta}-(n-\iota)^{\eta}\right)\Lambda_h - \left(\frac{(\beta_2 V_{\iota}+\beta_3\kappa D_{\iota}+\beta_4 I_{\iota})S_{\iota}}{N_{h\iota}} - \mu_h S_{\iota} + \gamma R_{\iota}\right),\\
I_{n+1} &= I_0 + \frac{\mathfrak{h}^{\eta}}{\Gamma(\eta+1)}\sum_{\iota=0}^{n}\left((n+1-\iota)^{\eta}-(n-\iota)^{\eta}\right)\times\left(\frac{(\beta_2 V_{\iota}+\beta_3\kappa D_{\iota}+\beta_4 I_{\iota})S_{\iota}}{N_{h\iota}} - q_1 I_{\iota}\right),\\
H_{n+1} &= H_0 + \frac{\mathfrak{h}^{\eta}}{\Gamma(\eta+1)}\sum_{\iota=0}^{n}\left((n+1-\iota)^{\eta}-(n-\iota)^{\eta}\right)\left(\rho I_{\iota} - q_2 H_{\iota}\right),\\
R_{n+1} &= R_0 + \frac{\mathfrak{h}^{\eta}}{\Gamma(\eta+1)}\sum_{\iota=0}^{n}\left((n+1-\iota)^{\eta}-(n-\iota)^{\eta}\right)\left(\alpha_1 I_{\iota} + \sigma H_{\iota} - q_3 R_{\iota}\right),\\
D_{n+1} &= D_0 + \frac{\mathfrak{h}^{\eta}}{\Gamma(\eta+1)}\sum_{\iota=0}^{n}\left((n+1-\iota)^{\eta}-(n-\iota)^{\eta}\right)\left(q_4 I_{\iota} - \nu D_{\iota}\right).
\end{aligned}
\tag{44}
$$

5.2. Simulation Predicting the Dynamics of NiV. This section presents the simulation of the Caputo NiV epidemic model (17) using the aforementioned numerical procedure obtained in (44). The time interval is taken in days. The parameter values are given in Table 1. The NiV model (17) simulation is performed for two cases and for the different fractional order of $\eta \in (0, 1]$.

Case 12. In the first case, the parameters are set such that $\mathscr{R}_0 > 1$. This case considers the parameter values to its baseline values as given in Table 1. The dynamics of viral concentration in foods, susceptible flying foxes, and infected flying foxes for both integer and fractional values of the parameter η are illustrated in plot Figures 1(a)–1(c). The dynamic features of susceptible, infectious, hospitalized recovered, and deceased humans are illustrated for various values of the fractional order η in Figures 2(a)–2(e), respectively. These plots revealed the convergence of solution curves to the endemic equilibrium for all values of η. This means that the epidemic reaches a stable equilibrium where the virus persists at a low level in the population, but the disease continues to circulate.

Case 13. In this scenario, some of the parameters are perturbed in order to simulate the model for the case when $\mathscr{R}_0 < 1$. We slightly changed some of the parameters while the rest remained the same as given in Table 1. We consider that $\beta_1 = 0.25, \beta_2 = 0.25, \beta_3 = 0.15, \beta_4 = 0.35$, and $\mu_f = 0.25$. The simulation for virus concentration and flying foxes population for Case 13 are presented in Figures 3(a)–3(c), while the human population dynamics are demonstrated in Figures 4(a)–4(d), respectively. The graphical results in this case confirm the convergence of the infection-free equilibrium state of the NiV fractional epidemic model for all values of η.

6. Dynamics of NiV Infection in Fractal-Fractional Perspective

This section further extends the NiV epidemic model using the generalized FF operator in the Caputo sense. To establish the desired problem, we replace the fractional derivative in model (17) by the FF operator with fractal and fractional parameters, respectively, denoted by ϑ and η. The generalized NiV epidemic model with this novel modeling approach can be described as follows:

Table 1: Numerical values of the system parameters used in numerical results.

Parameters	Physical meaning	Value	Source
Λ_h	Recruitment rate of human class	6295.16	[26]
Λ_f	Recruitment rate of flying foxes class	300	[35]
μ_h	Natural mortality in humans	$1/365 \times 73.57$	[26]
μ_f	Natural mortality in flying foxes	0.025	[35]
ν	Cremation/burial rate of deceased bodies	0.5	[36]
p	Virus shedding rate in F_i	0.100	Assumed
θ	Viral decay rate	0.09	Assumed
γ	Rate of immunity losses in recovered human	0.85	[36]
β_1	Rate at which S_f becomes infected	0.50	Assumed
β_2	Rate at which S becomes infected	0.65	[35]
β_3	Unsafe contact rate of S class with deceased bodies	0.75	[36]
β_4	Unsafe contact rate of S class with infectious human	0.65	[36]
α_1	Recovery rate in I	0.09	[36]
α_2	Disease-induced death rate in infected human class	0.77	[35]
μ_1	Disease-induced death rate in hospitalized class	0.387	[37]
ρ	Hospitalization rate of infected human individuals	0.4	[37]
σ	Recovery rate of hospitalized class	0.09	[37]
κ	Fraction of dead bodies which are handled unsafely	0.001	[35]

$$
\begin{aligned}
{}^{FF}D_{0,t}^{\eta,\vartheta}(V(t)) &= pI_f - \theta V,\\
{}^{FF}D_{0,t}^{\eta,\vartheta}\left(S_f(t)\right) &= \Lambda_f - \frac{\beta_1 S_f V}{N_f} - \mu_f S_f,\\
{}^{FF}D_{0,t}^{\eta,\vartheta}\left(I_f(t)\right) &= \frac{\beta_1 S_f V}{N_f} - \mu_f I_f,\\
{}^{FF}D_{0,t}^{\eta,\vartheta}(S(t)) &= \Lambda_h - \frac{(\beta_2 V + \kappa\beta_3 D + \beta_4 I)S}{N_h} - \mu_h S + \gamma R,\\
{}^{FF}D_{0,t}^{\eta,\vartheta}(I(t)) &= \frac{(\beta_2 V + \kappa\beta_3 D + \beta_4 I)S}{N_h} - q_1 I,\\
{}^{FF}D_{0,t}^{\eta,\vartheta}(H(t)) &= \rho I - q_2 H,\\
{}^{FF}D_{0,t}^{\eta,\vartheta}(R(t)) &= \alpha_1 I + \sigma H - q_3 R,\\
{}^{FF}D_{0,t}^{\eta,\vartheta}(D(t)) &= q_4 I - \nu D,
\end{aligned}
\tag{45}
$$

where ${}^{FF}D_{0,t}^{\eta,\vartheta}$ is the Caputo fractal-fractional operator. In further study, we illustrate the basic necessary properties of the FF case model (45).

6.1. Uniqueness and Existence. The uniqueness and existence of the considered FF problem are the necessary mathematical properties. Therefore, this section proves the aforementioned feature of the NiV epidemic model in the fractal-fractional case (45). The widely used Picard–Lindelöf theorem of a fixed-point approach is considered for the said result. In order to achieve the desired goal, FF in (45) is described as a general Cauchy problem in the following system:

$$
\begin{cases}
{}^{FF}D_{0,t}^{\eta,\vartheta} f(t) = \mathcal{G}(t, f(t)),\\
f(0) = f_0, \quad 0 < t < \mathcal{T} < \infty.
\end{cases}
\tag{46}
$$

In problem (46), the function describing the state variable is $f(t) = (V, S_f, I_f, S, I, H, R, D)$ and $\mathcal{G}$ describes the ad continuous vector function as described in the previous part. Moreover, the initial condition for the abovementioned Cauchy problem is denoted by

$$
f_0 = \left(V(0), S_f(0), I_f(0), S(0), I(0), H(0), R(0), D(0)\right).
\tag{47}
$$

The application of integral in FF case over the Cauchy problem (46) leads to the following form:

$$
\frac{1}{\Gamma(1-\eta)}\frac{d}{dt}\int_0^t (t-\varsigma)^{-\eta}\mathcal{G}(t, f(t))d\varsigma = \vartheta t^{\vartheta-1}\mathcal{G}(t, f(t)).
\tag{48}
$$

The right side in the abovementioned equation is being replaced with the Caputo derivative, and after the application of integral, we get the following result [38]:

$$
f(t) = f(0) + \frac{\vartheta}{\Gamma(\eta)}\int_0^t (t-\varsigma)^{\eta-1}\varsigma^{\vartheta-1}\mathcal{G}(\varsigma, g(\varsigma))d\varsigma.
\tag{49}
$$

Keeping the Picard–Lindelöf theorem in view, we present the following definition:

$$
\prod_a^b = \mathcal{J}_n(t_n) \times \overline{\mathbb{B}_0(p_0)},
\tag{50}
$$

such that

$$
\begin{aligned}
\mathcal{J}_n(t_n) &= [t_{n-a}, t_{n+a}],\\
\overline{\mathbb{B}_0(p_0)} &= [b + t_0, t_0 + b].
\end{aligned}
\tag{51}
$$

In addition, we define the operator as

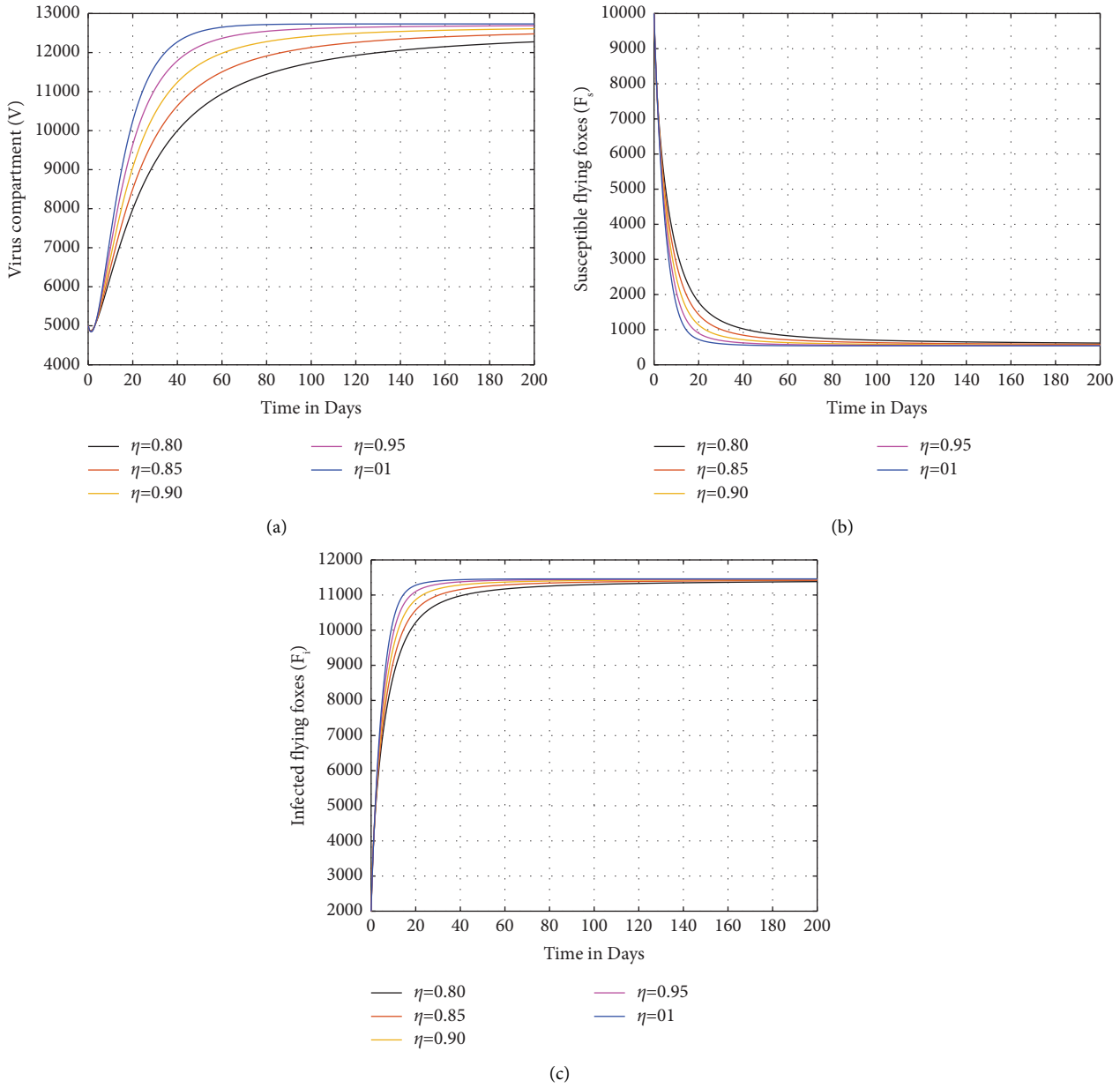

FIGURE 1: Simulation of (a) the virus compartment $V(t)$, (b) susceptible flying foxes $S_f(t)$, and (c) infected flying foxes $I_f(t)$ in the fractional NiV transmission model (17) with $\eta = 1.0, 0.95, 0.90, 0.85, 0.80$. The parameter values are mentioned in Table 1 and $\mathscr{R}_0 > 1$.

$$\Lambda.C\left[\mathscr{I}_n(t_n), \mathbb{B}_b(t_n)\right] \longrightarrow C\left(\mathscr{I}_n(t_n), \mathbb{A}_b(t_n)\right), \tag{52}$$

such that

$$\Lambda\phi(t) = f(0) + \frac{\vartheta}{\Gamma(\eta)} \int_0^t (t-\varsigma)^{\eta-1} \varsigma^{\vartheta-1} \mathscr{G}(\varsigma, \phi(\varsigma)) \mathrm{d}\varsigma. \tag{53}$$

In the onward proof, we will focus on proving that the operator given in (53) maps a complete norm empty metric space over self. In addition, the essential fact is to confirm that the map has a contraction property. In the first attempt, we prove that

$$\|\Lambda\phi(t) - f(0)\| \leq c. \tag{54}$$

The following norm is taken into account:

$$\begin{aligned} \|\Lambda\phi(t) - f(0)\| &\leq \frac{\vartheta}{\Gamma(\eta)} \int_0^t (t-\varsigma)^{\eta} \varsigma^{\vartheta-1} \|\mathscr{G}(\varsigma, f(\varsigma))\|_{\infty} \mathrm{d}\varsigma \\ &\leq \frac{\vartheta}{\Gamma(\eta)} \mathscr{H} \int_0^t (t-\varsigma)^{\eta} \varsigma^{\vartheta-1} \mathrm{d}\varsigma, \end{aligned} \tag{55}$$

with

$$\mathscr{H} = \|\mathscr{G}\|_{\infty}, \tag{56}$$

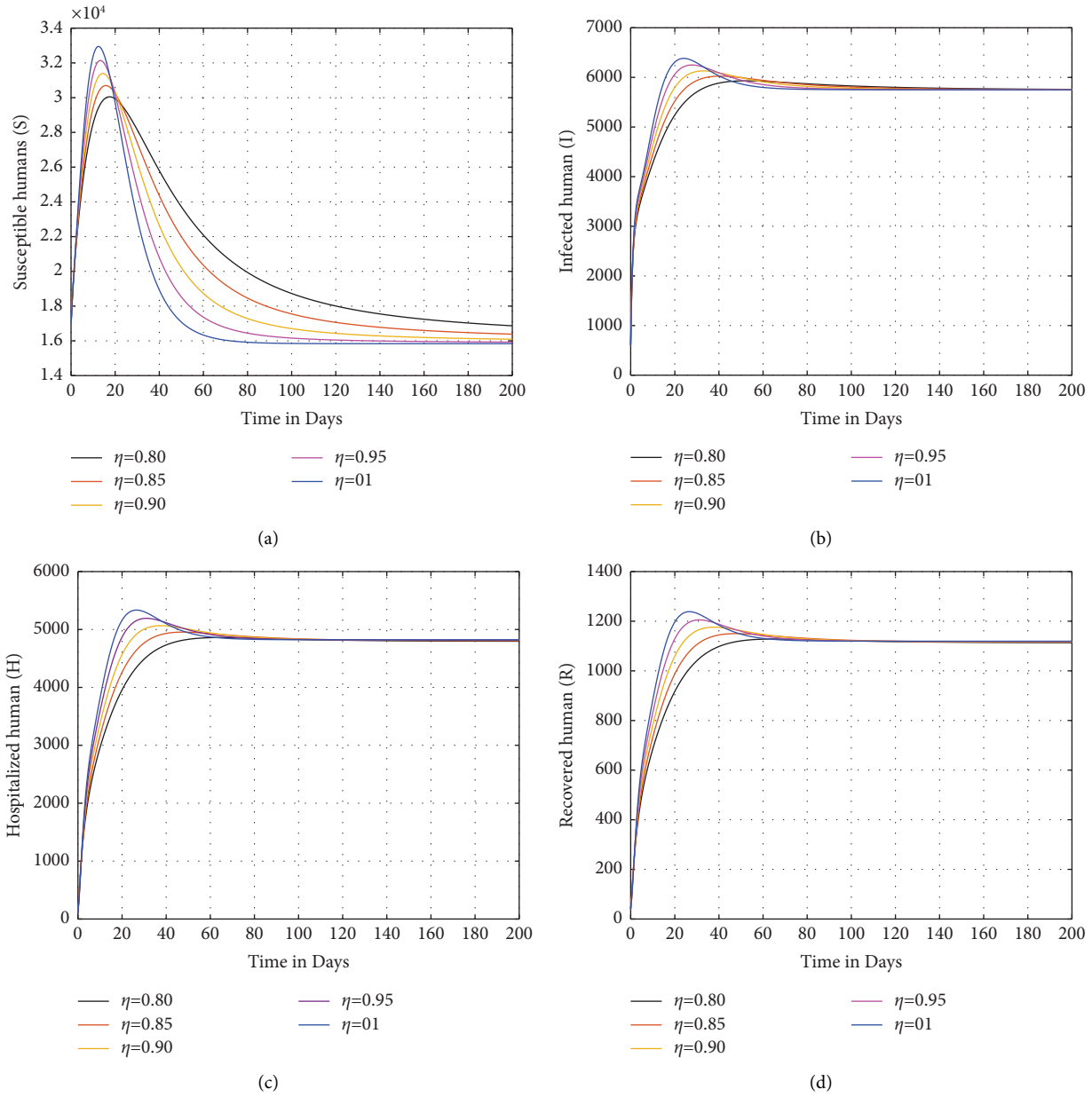

Figure 2: Continued.

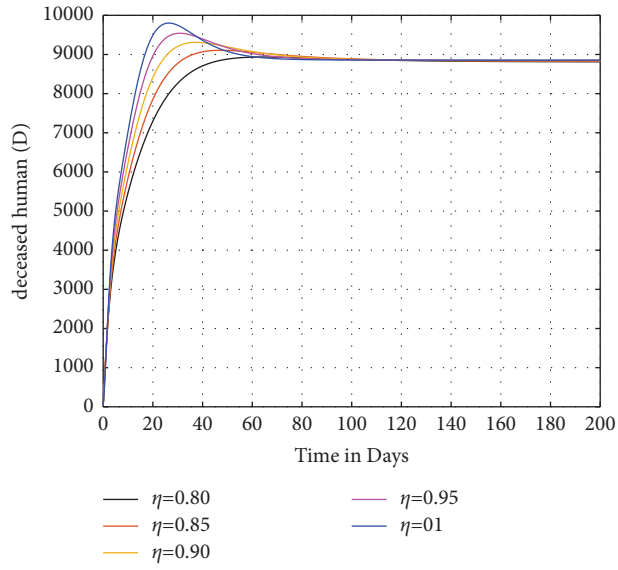

(e)

Figure 2: Simulation of (a) susceptible humans $S(t)$, (b) infected humans $I(t)$, (c) hospitalized humans $H(t)$, (d) recovered humans $R(t)$, and (e) deceased humans D in the fractional NiV transmission model (17) with $\eta = 1.0, 0.95, 0.90, 0.85, 0.80$. The parameter values are mentioned in Table 1 and $\mathscr{R}_0 > 1$.

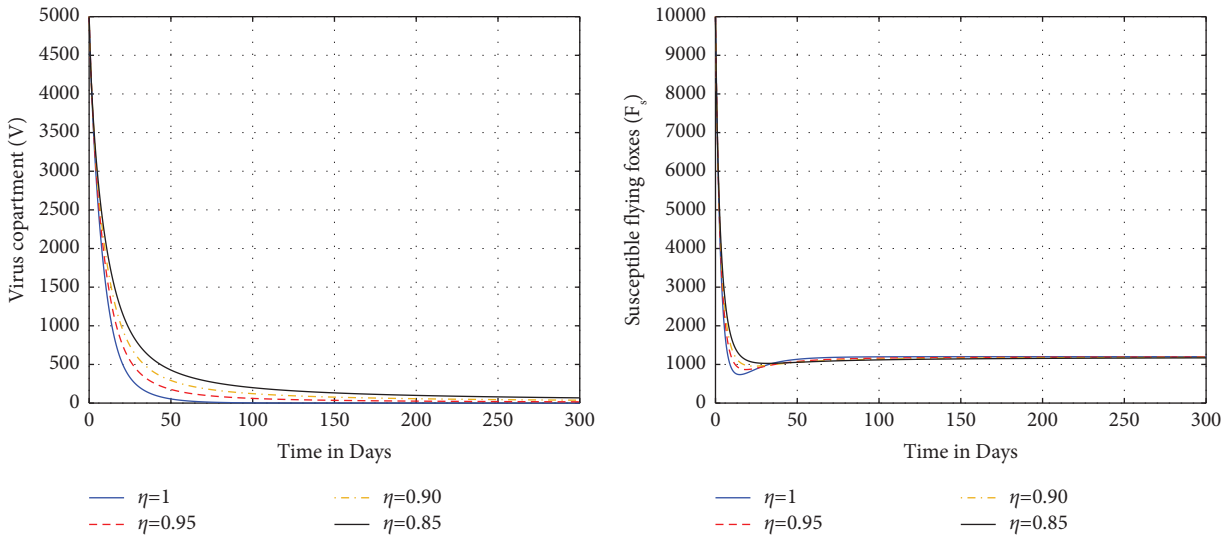

(a) (b)

Figure 3: Continued.

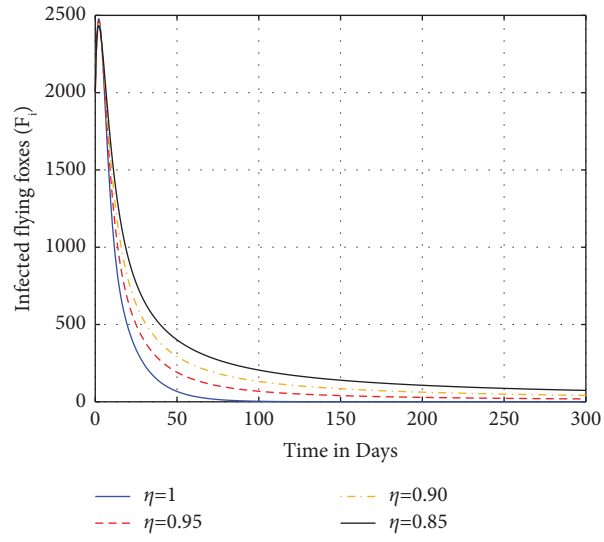

(c)

Figure 3: Simulation of (a) the virus compartment $V(t)$, (b) susceptible flying foxes $S_f(t)$, and (c) infected flying foxes $I_f(t)$ in the fractional NiV transmission model (17) with $\eta = 1.0, 0.95, 0.90, 0.85$. The parameter values are mentioned in Table 1 and $\mathscr{R}_0 < 1$.

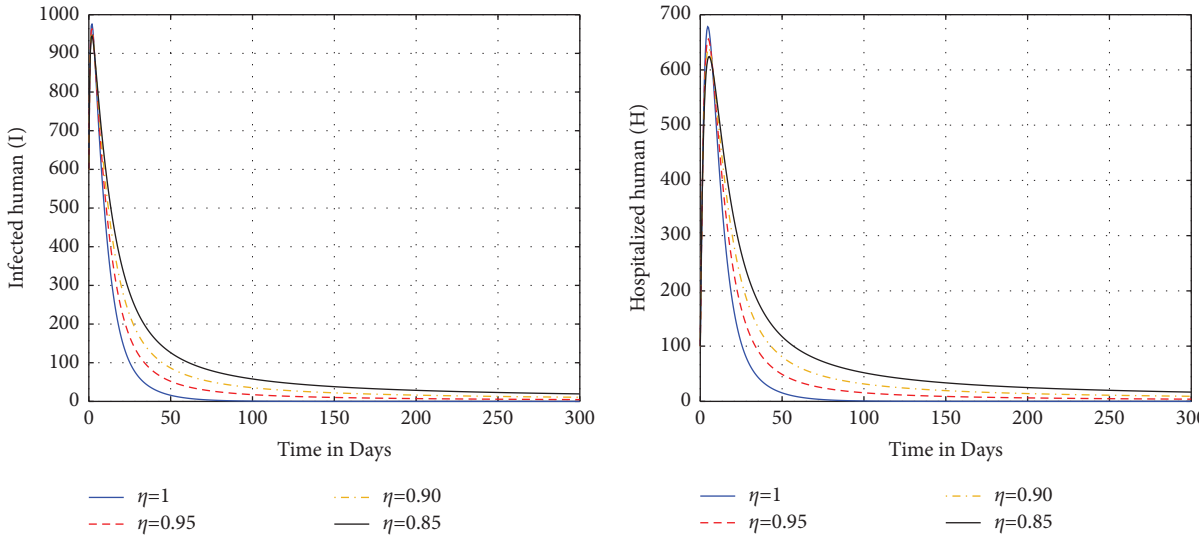

(a) (b)

Figure 4: Continued.

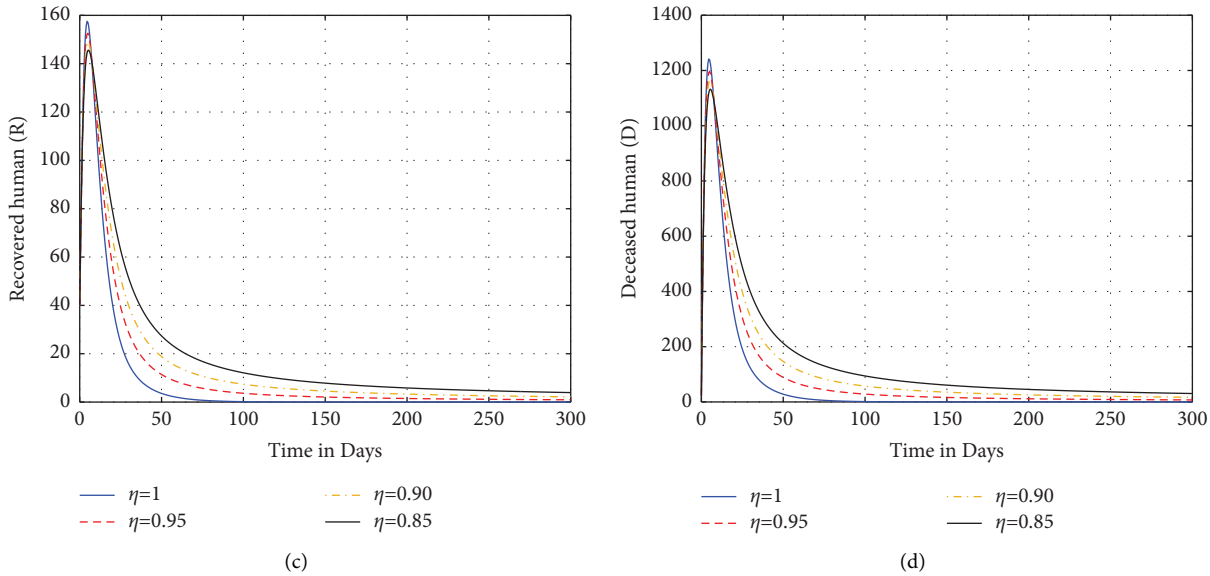

FIGURE 4: Simulation of (a) infected humans $I(t)$, (b) hospitalized humans $I(t)$, (c) recovered humans $R(t)$, and (d) deceased humans D in the fractional NiV transmission model (17) with $\eta = 1.0, 0.95, 0.90, 0.85$. The parameter values are mentioned in Table 1 and $\mathscr{R}_0 < 1$.

where the norm is given by

$$\|\Theta\|_{\infty} = \sup_{t\in\prod_a^b}\|\Theta(t)\|. \tag{57}$$

Moreover, let us suppose that $\varsigma = ty$, then from the abovementioned integral, we have

$$\begin{aligned}\|\Lambda\phi(t) - f(0)\| &\leq \frac{\vartheta\mathscr{H}}{\Gamma(\eta)}t^{\eta+\vartheta-1}B(\eta,\vartheta),\\ \|\Lambda\phi(t) - f(0)\| < c &\Longleftrightarrow \mathscr{H} < \frac{c\Gamma(\eta)}{\vartheta a^{\vartheta+\eta-1}B(\eta,\vartheta)}.\end{aligned} \tag{58}$$

By considering ϕ_1 and $\phi_2 \in C[\mathscr{J}_n(t_n), \mathbb{B}_b(t_n)]$, the inequity is obtained as

$$\begin{aligned}\|\Lambda\phi_1 - \Lambda\phi_2\| &\leq \left(\frac{\vartheta\mathscr{H}}{\Gamma(\eta)}t^{\vartheta+\eta-1}B(\eta,\vartheta)\right)\|\phi_1 - \phi_2\|\\ &< \left(\frac{\vartheta\mathscr{H}}{\Gamma(\eta)}a^{\vartheta+\eta-1}B(\eta,\vartheta)\right)\|\phi_1 - \phi_2\|.\end{aligned} \tag{59}$$

Finally, from the abovementioned equation, we deduce the contraction property under the condition that if the following criteria are fulfilled, then we get

$$\mathscr{H} < \frac{\Gamma(\eta)}{\vartheta a^{\vartheta+\eta-1}B(\eta,\vartheta)}. \tag{60}$$

6.2. Numerical Solution for the FF NiV Model. The numerical schemes for the nonlinear complex problem are necessary to illustrate the dynamical aspect of the problem under consideration graphically. This section provides a numerical procedure for the FF NiV epidemic model (45). The novel numerical procedure-based Lagrangian piecewise polynomial interpolation is applied to derive the iterative scheme of system (45) [38, 39]. The FF model (45) is rewritten in the Volterra-type due to the differentiability of the fractional integral operator. Moreover, the FF problem in the RL operator case can be described as

$$\left(\frac{1}{\Gamma(1-\eta)}\right)\frac{d}{dt}\int_0^t (t-\varsigma)^{-\eta}f(\varsigma)d\varsigma\frac{1}{\vartheta t^{\vartheta-1}}. \tag{61}$$

Therefore, problem (46) can be converted as

$${}^{RL}D_{0,t}^{\eta}(f(t)) = \vartheta t^{\vartheta-1}[\mathscr{G}(t, f(t))]. \tag{62}$$

Moreover, the derivative in the RL sense is replaced by the Caputo-type operator in order to implement the integer-order ICs. As a result, (62) can be expressed as

$$f(t) = f(0) + \frac{\vartheta}{\Gamma(\eta)}\int_0^t \varsigma^{\vartheta-1}(t-\varsigma)^{\eta-1}\mathscr{G}(\varsigma, p(\varsigma))d\varsigma. \tag{63}$$

Now at $t = t_{n+1}$, (63) gets the following form:

$$\begin{aligned}f^{n+1} &= f_0 + \frac{\vartheta}{\Gamma(\eta)}\int_0^{t_{n+1}}\varsigma^{\vartheta-1}(t_{n+1}-\varsigma)^{\eta-1}\mathscr{G}(\varsigma, f)d\varsigma\\ &= f_0 + \frac{\vartheta}{\Gamma(\eta)}\sum_{\nu=0}^{n}\int_{t_\nu}^{t_{\nu+1}}\varsigma^{\vartheta-1}(t_{n+1}-\varsigma)^{\eta-1}\mathscr{G}(\varsigma, f(\varsigma))d\varsigma.\end{aligned} \tag{64}$$

Furthermore, $\mathscr{G}(\varsigma, f(\varsigma))$ in (64) is approximated by making use of the Lagrangian piecewise interpolation approach over $[t_j, t_{j+1}]$ as

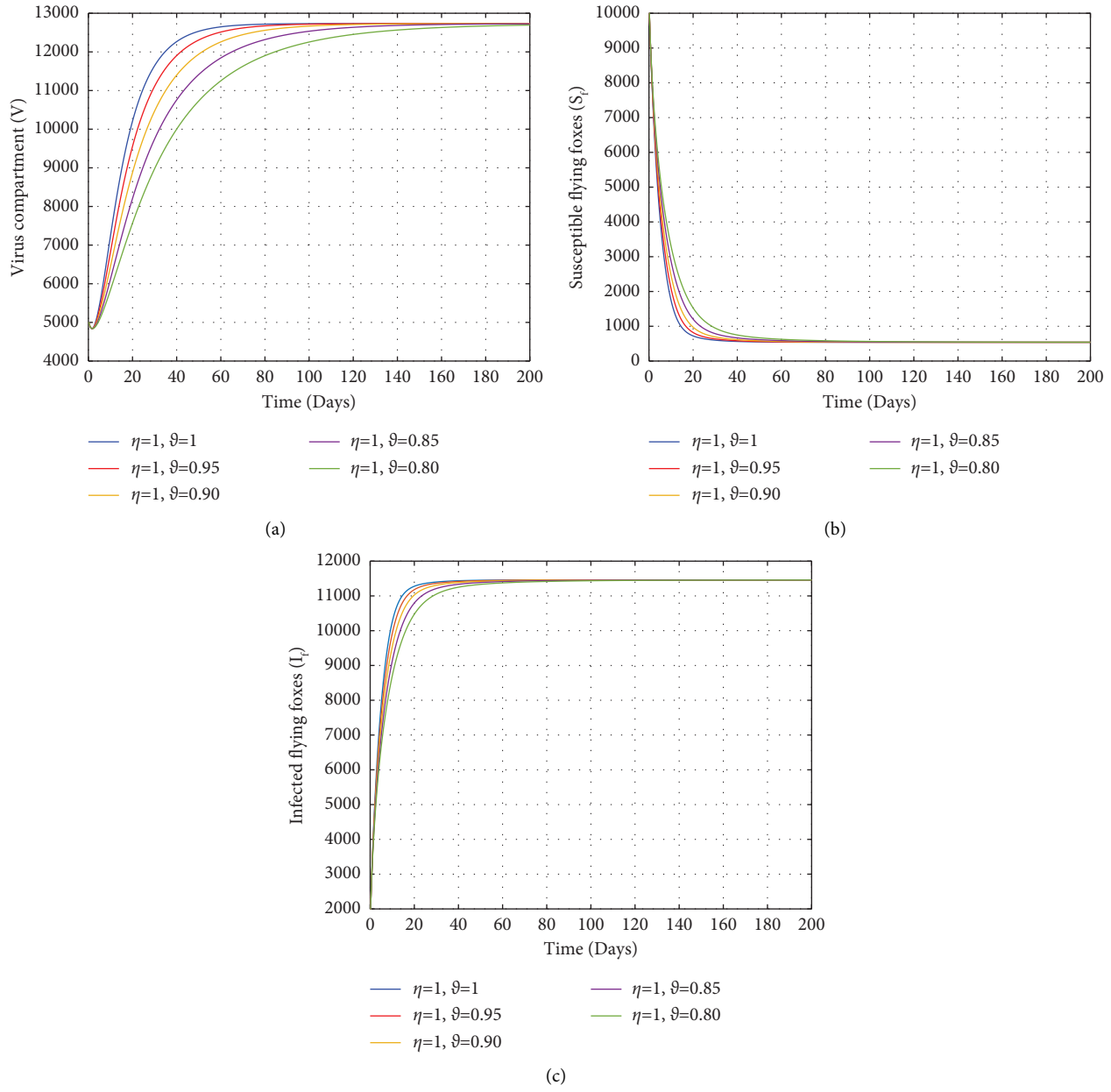

Figure 5: Case 14: the dynamics of the FF NiV epidemic model (45) when $\vartheta = 1.00, 0.95, 0.90, 0.80, 0.85$ and $\eta = 1$: (a) virus concentration (b) susceptible flying foxes, and (c) infected flying foxes.

$$\mathcal{G}(\varsigma, f(\varsigma)) \approx f_j(\varsigma) = \frac{\varsigma - t_{j-1}}{t_j - t_{j-1}} t_j^{\vartheta-1} \mathcal{G}\left(t_j, f\left(t_j\right)\right) - \frac{\varsigma - t_j}{t_j - t_{j-1}} t_{j-1}^{\vartheta-1} \mathcal{G}\left(t_{j-1}, f\left(t_{j-1}\right)\right). \tag{65}$$

We lead to the following expression after making use of the aforementioned approximation:

$$f^{n+1} = f_0 + \frac{\vartheta}{\Gamma(\eta)} \sum_{j=0}^{n} \int_{t_j}^{t_{j+1}} \lambda^{\vartheta-1} \left(t_{n+1} - \varsigma\right)^{\eta-1} f_j(\varsigma) \mathrm{d}\varsigma. \tag{66}$$

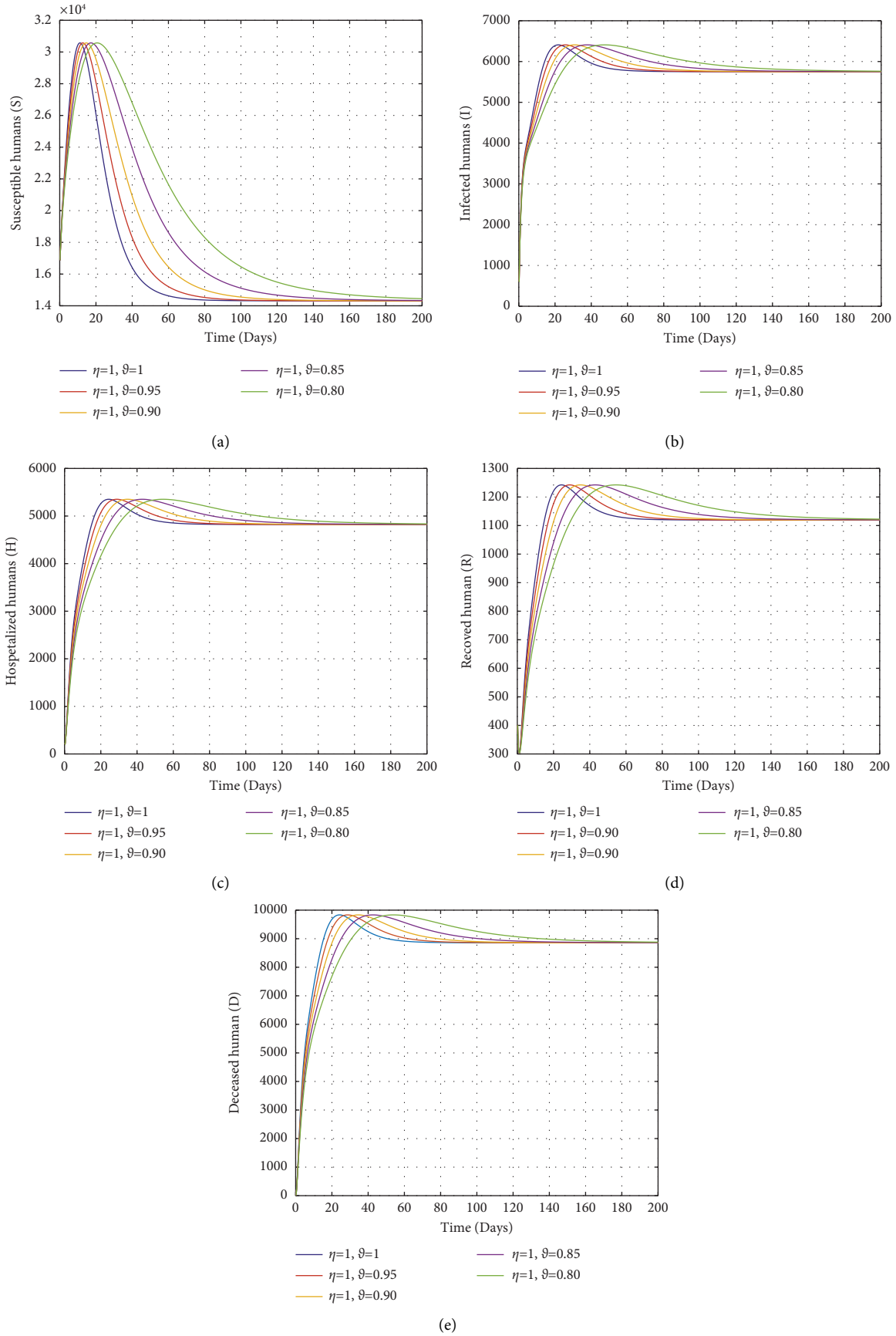

Figure 6: Case 14: the dynamics of the FF NiV epidemic model (45) when $\vartheta = 1.00, 0.95, 0.90, 0.80, 0.85$ and $\eta = 1$: (a) susceptible, (b) infectious, (c) hospitalized, (d) recovered, and (e) deceased humans.

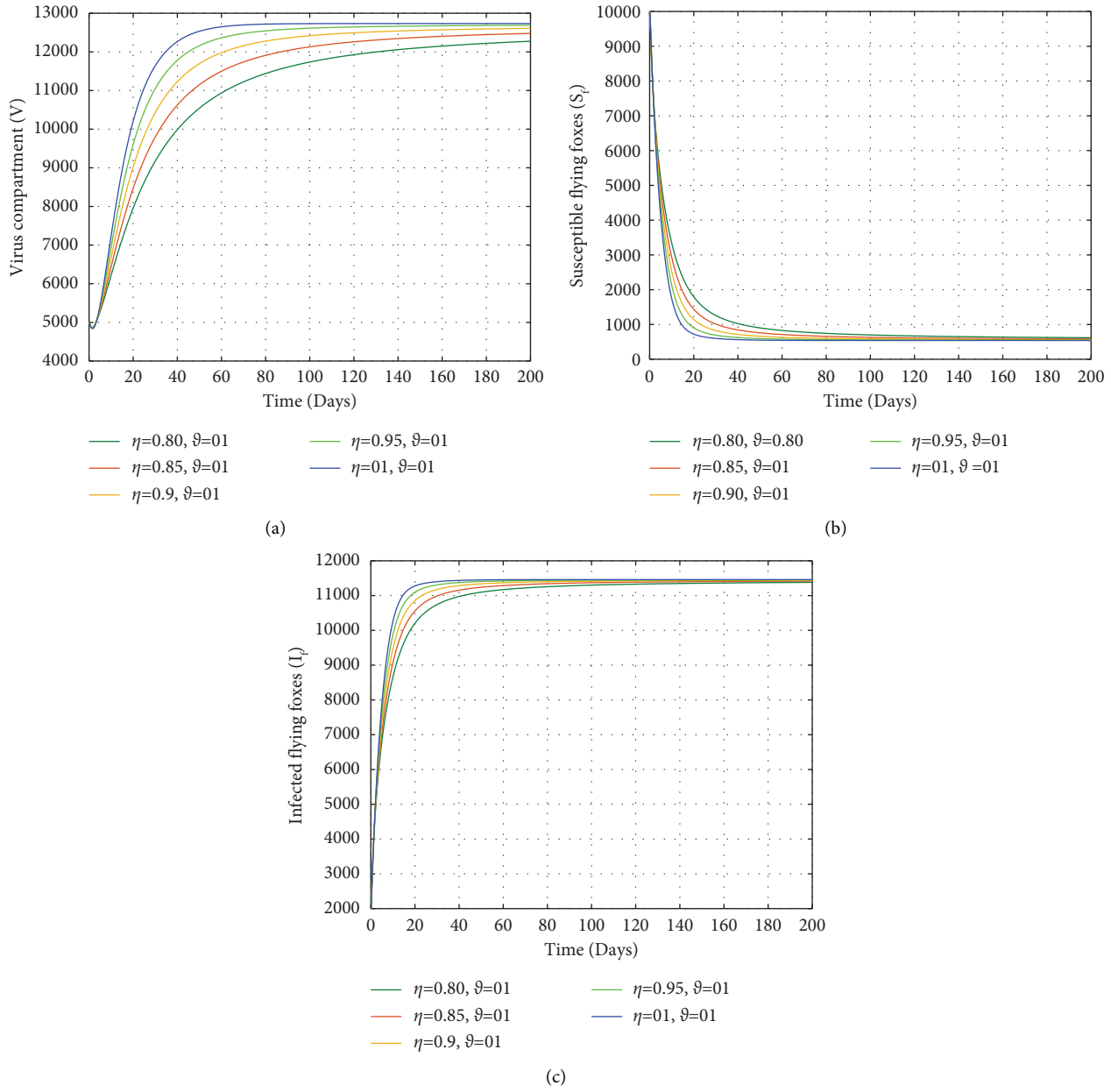

FIGURE 7: Case 15: the dynamics of the FF NiV epidemic model (45) when $\eta = 1.00, 0.95, 0.90, 0.80, 0.85$ and $\vartheta = 1$: (a) virus concentration, (b) susceptible flying foxes, and (c) infected flying foxes.

Finally, the solution of (66) provides the following iterative formulae:

$$f^{n+1} = f^0 + \frac{\vartheta \mathfrak{h}^\eta}{\Gamma(\eta+2)} \sum_{\jmath=0}^{n} \Big[t_\jmath^{\vartheta-1} \mathcal{G}\big(t_\jmath, g(t_\jmath)\big) \times \big((1+n-\jmath)^\eta (n+2-\jmath+\eta) - (n-\jmath)^\eta (n+2-\jmath+2\eta)\big) - t_{\jmath-1}^{\vartheta-1} \mathcal{G}\big(t_{\jmath-1}, g(t_{\jmath-1})\big) \times \big((1+n-\jmath)^{\eta+1} - (n-\jmath)^\eta (n-\jmath+1+\eta)\big) \Big]. \tag{67}$$

The desired iterative formulae are established as follows for the FF NiV epidemic model (45):

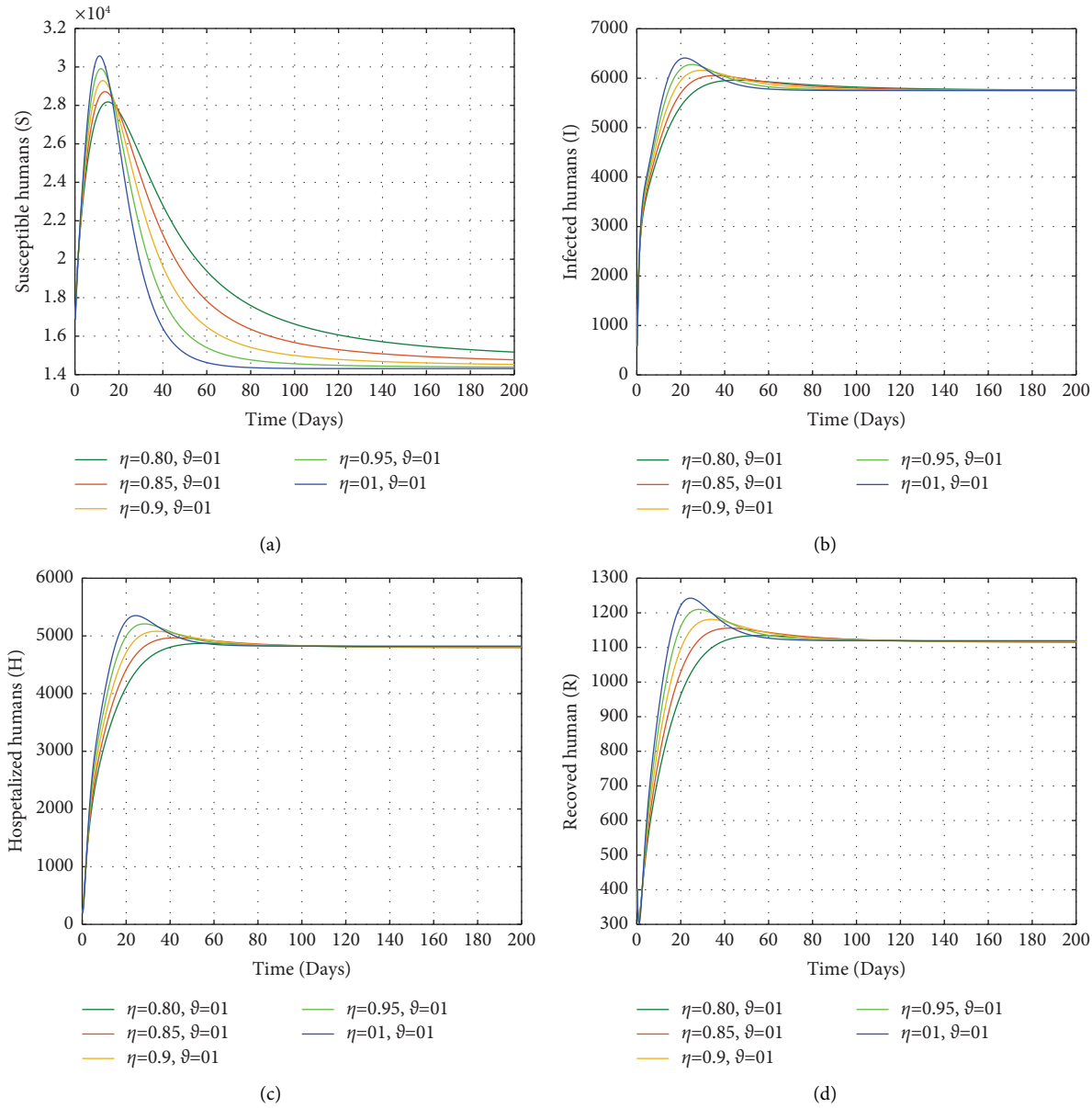

Figure 8: Continued.

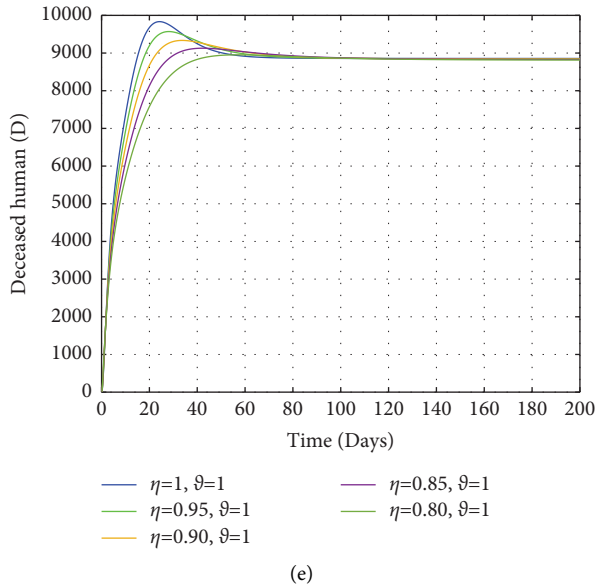

FIGURE 8: Case 15: the dynamics of the FF NiV epidemic model (45) when $\eta = 1.00, 0.95, 0.90, 0.80, 0.85$ and $\vartheta = 1$ (a) susceptible, (b) infectious, (c) hospitalized, (d) recovered, and (e) deceased humans.

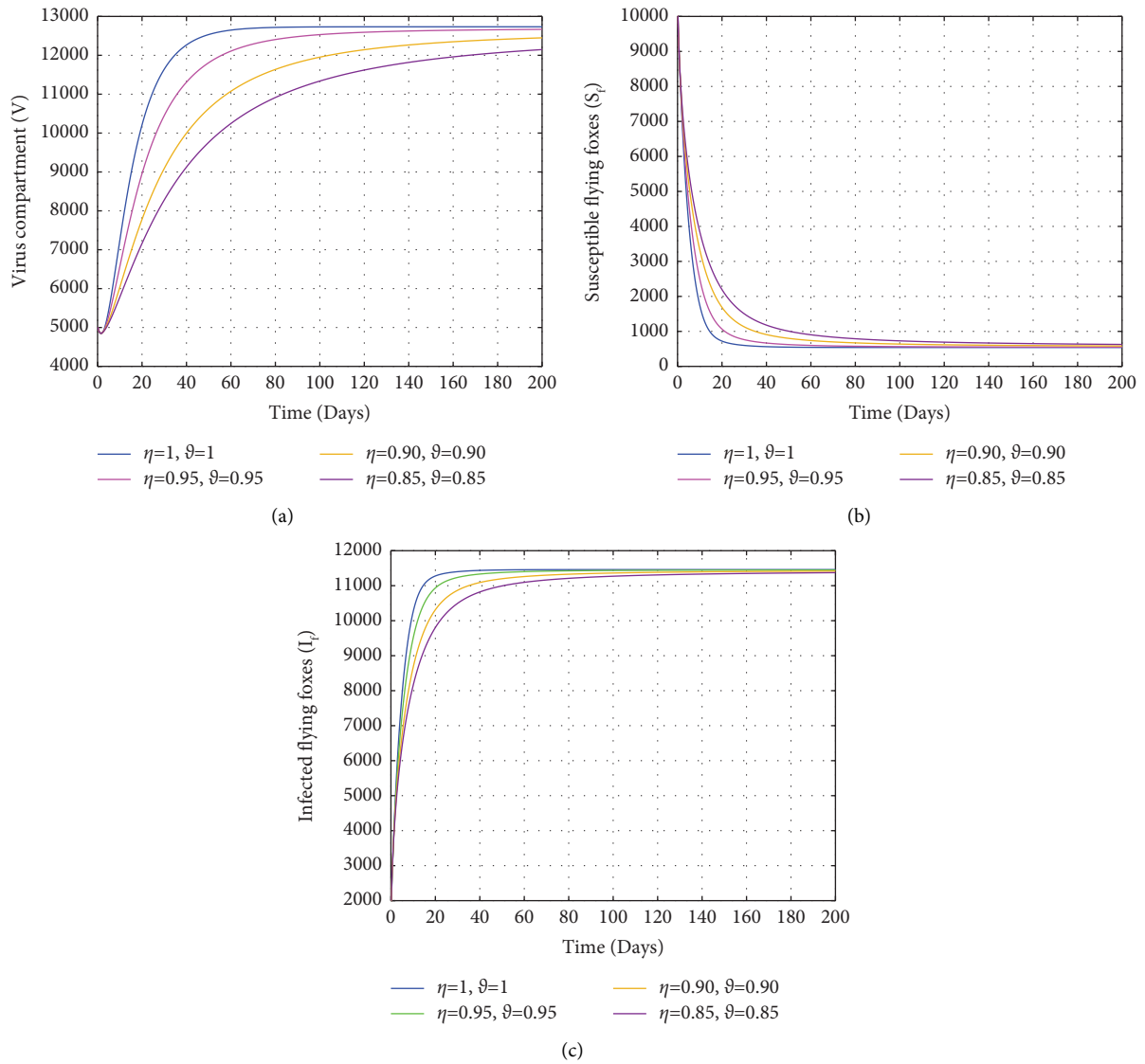

FIGURE 9: Case 16: the dynamics of the FF NiV epidemic model (45) when $\eta = 1.00, 0.95, 0.90, 0.85$ and $\vartheta = 1.00, 0.95, 0.90, 0.85$: (a) virus concentration, (b) susceptible flying foxes, and (c) infected flying foxes.

$$
\begin{aligned}
V^{n+1} &= V^0 + \frac{\vartheta \mathfrak{h}^\eta}{\Gamma(\eta+2)} \sum_{\jmath=0}^{n} \Big[t_\jmath^{\vartheta-1} \mathcal{G}_1\big(t_\jmath, f(t_\jmath)\big) \\
&\quad \times \big((1+n-\jmath)^\eta (n+2+\eta-\jmath) - (n-\jmath)^\eta (n+2-\jmath+2\eta) \big) \\
&\quad - t_{\jmath-1}^{\vartheta-1} \mathcal{G}_1\big(t_{\jmath-1}, f(t_{\jmath-1})\big) \times \big((1+n-\jmath)^{\eta+1} - (n-\jmath)^\eta (n+1-\jmath+\eta) \big) \Big], \\
S_f^{n+1} &= S_f^0 + \frac{\vartheta \mathfrak{h}^\eta}{\Gamma(\eta+2)} \sum_{\jmath=0}^{n} \Big[t_\jmath^{\vartheta-1} \mathcal{G}_2\big(t_\jmath, f(t_\jmath)\big) \\
&\quad \times \big((1+n-\jmath)^\eta (n+2+\eta-\jmath) - (n-\jmath)^\eta (n-\jmath+2+2\eta) \big) \big) \\
&\quad - t_{\jmath-1}^{\vartheta-1} \mathcal{G}_2\big(t_{\jmath-1}, f(t_{\jmath-1})\big) \times \big((n+1-\jmath)^{\eta+1} - (n-\jmath)^\eta (n+1-\jmath+\eta) \big) \Big], \\
I_f^{n+1} &= I_f^0 + \frac{\vartheta \mathfrak{h}^\eta}{\Gamma(\eta+2)} \sum_{\jmath=0}^{n} \Big[t_\jmath^{\vartheta-1} \mathcal{G}_3\big(t_\jmath, f(t_\jmath)\big) \\
&\quad \times \big((1+n-\jmath)^\eta (n+2+\eta-\jmath) - (n-\jmath)^\eta (n+2-\jmath+2\eta) \big) \\
&\quad - t_{\jmath-1}^{\vartheta-1} \mathcal{G}_3\big(t_{\jmath-1}, f(t_{\jmath-1})\big) \times \big((n+1-\jmath)^{\eta+1} - (n-\jmath)^\eta (n+1-\jmath+\eta) \big) \Big], \\
S^{n+1} &= S^0 + \frac{\vartheta \mathfrak{h}^\eta}{\Gamma(\eta+2)} \sum_{\jmath=0}^{n} \Big[t_\jmath^{\vartheta-1} \mathcal{G}_4\big(t_\jmath, f(t_\jmath)\big) \\
&\quad \times \big((1+n-\jmath)^\eta (n+2+\eta-\jmath) - (n-\jmath)^\eta (n+2-\jmath+2\eta) \big) \\
&\quad - t_{\jmath-1}^{\vartheta-1} \mathcal{G}_4\big(t_{\jmath-1}, f(t_{\jmath-1})\big) \times \big((n+1-\jmath)^{\eta+1} - (n-\jmath)^\eta (n+1-\jmath+\eta) \big) \Big], \\
I^{n+1} &= I^0 + \frac{\vartheta \mathfrak{h}^\eta}{\Gamma(\eta+2)} \sum_{\jmath=0}^{n} \Big[t_\jmath^{\vartheta-1} \mathcal{G}_5\big(t_\jmath, f(t_\jmath)\big) \\
&\quad \times \big((1+n-\jmath)^\eta (n+2+\eta-\jmath) - (n-\jmath)^\eta (n+2-\jmath+2\eta) \big) \\
&\quad - t_{\jmath-1}^{\vartheta-1} \mathcal{G}_5\big(t_{\jmath-1}, f(t_{\jmath-1})\big) \times \big((n+1-\jmath)^{\eta+1} - (n-\jmath)^\eta (n+1-\jmath+\eta) \big) \Big], \\
H^{n+1} &= H^0 + \frac{\vartheta \mathfrak{h}^\eta}{\Gamma(\eta+2)} \sum_{\jmath=0}^{n} \Big[t_\jmath^{\vartheta-1} \mathcal{G}_6\big(t_\jmath, f(t_\jmath)\big) \\
&\quad \times \big((1+n-\jmath)^\eta (n+2+\eta-\jmath) - (n-\jmath)^\eta (n+2-\jmath+2\eta) \big) \\
&\quad - t_{\jmath-1}^{\vartheta-1} \mathcal{G}_6\big(t_{\jmath-1}, f(t_{\jmath-1})\big) \times \big((n+1-\jmath)^{\eta+1} - (n-\jmath)^\eta (n+1-\jmath+\eta) \big) \Big], \\
R^{n+1} &= R^0 + \frac{\vartheta \mathfrak{h}^\eta}{\Gamma(\eta+2)} \sum_{\jmath=0}^{n} \Big[t_\jmath^{\vartheta-1} \mathcal{G}_7\big(t_\jmath, f(t_\jmath)\big) \\
&\quad \times \big((1+n-\jmath)^\eta (n+2+\eta-\jmath) - (n-\jmath)^\eta (n+2-\jmath+2\eta) \big) \\
&\quad - t_{\jmath-1}^{\vartheta-1} \mathcal{G}_7\big(t_{\jmath-1}, f(t_{\jmath-1})\big) \times \big((n+1-\jmath)^{\eta+1} - (n-\jmath)^\eta (n+1-\jmath+\eta) \big) \Big], \\
D^{n+1} &= D^0 + \frac{\vartheta \mathfrak{h}^\eta}{\Gamma(\eta+2)} \sum_{\jmath=0}^{n} \Big[t_\jmath^{\vartheta-1} \mathcal{G}_8\big(t_\jmath, f(t_\jmath)\big) \\
&\quad \times \big((1+n-\jmath)^\eta (n+2+\eta-\jmath) - (n-\jmath)^\eta (n+2-\jmath+2\eta) \big) \\
&\quad - t_{\jmath-1}^{\vartheta-1} \mathcal{G}_8\big(t_{\jmath-1}, f(t_{\jmath-1})\big) \big((1+n-\jmath)^{\eta+1} - (n-\jmath)^\eta (n+\eta-\jmath+1) \big) \Big].
\end{aligned} \tag{68}
$$

6.3. Simulation of the FF NiV Model. This section illustrates an extensive simulation of the NiV compartmental model in the FF case (28) to analyze the influential effects of both fractal and fractional parameters on the problem dynamics. The numerical scheme derived in (68) is taken into account for the said purpose. Parameter values are considered from Table 1 with the same ICs taken for the fractional case model. We considered four cases in the

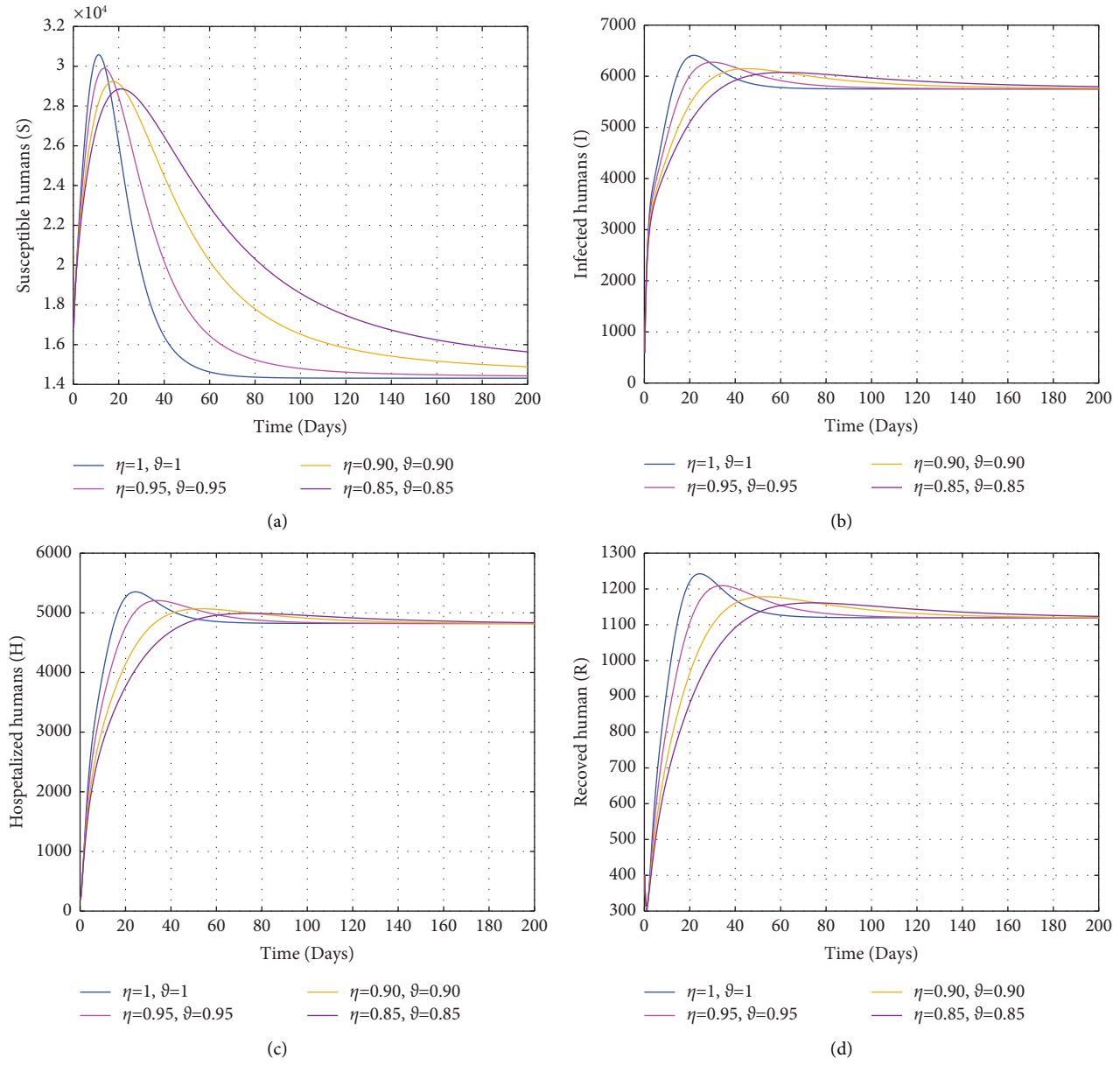

Figure 10: Continued.

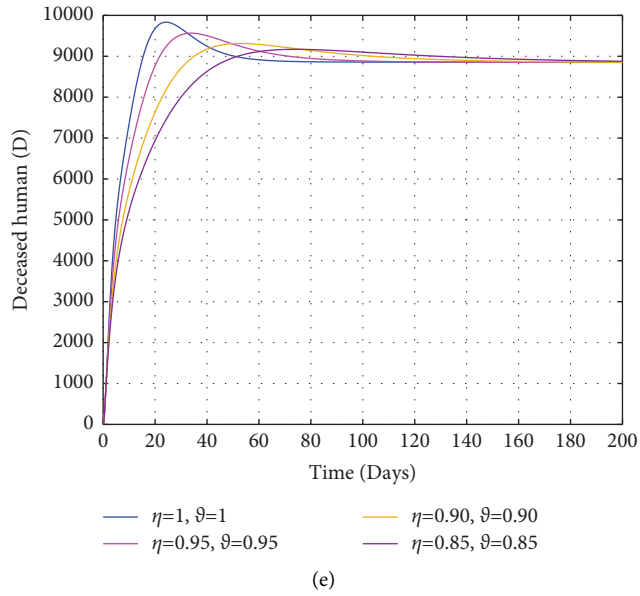

(e)

Figure 10: Case 16: the simulation of the FF NiV epidemic model (45) when $\eta = 1.00, 0.95, 0.90, 0.85$ and $\vartheta = 1.00, 0.95, 0.90, 0.85$: (a) susceptible, (b) infectious, (c) hospitalized, (d) recovered, and (e) deceased humans.

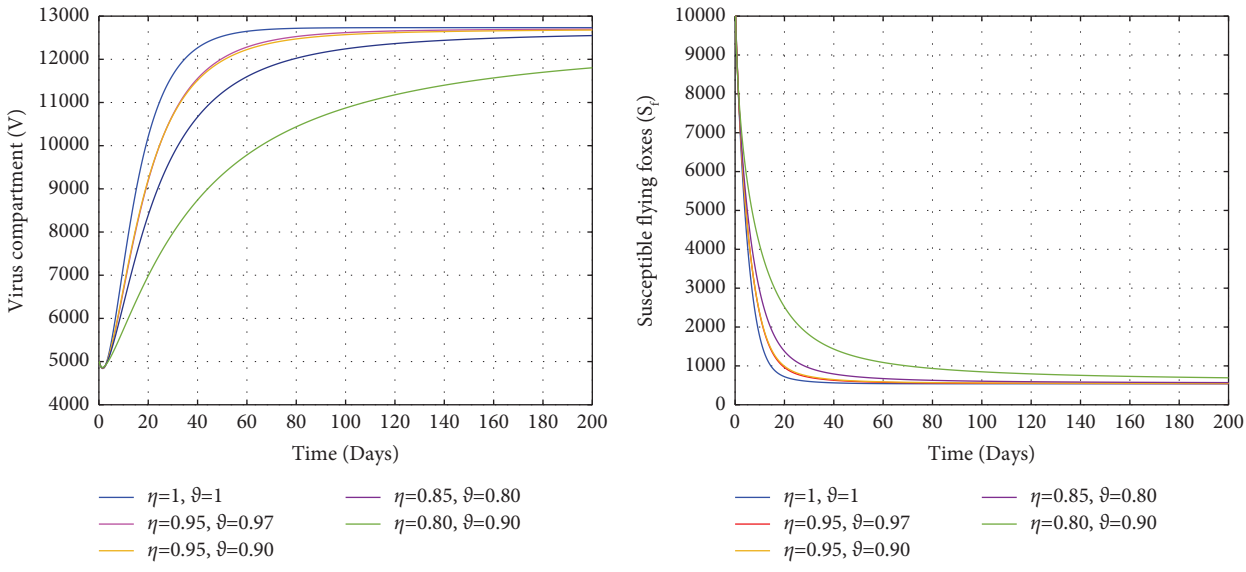

(a) (b)

Figure 11: Continued.

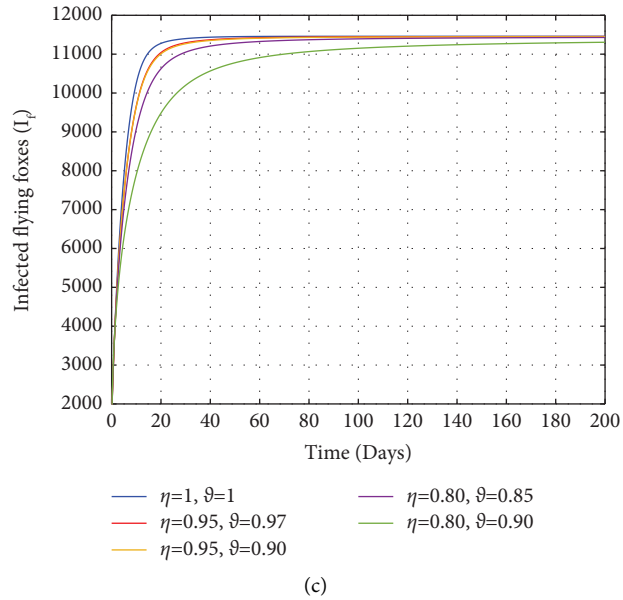

(c)

Figure 11: Case 17: the dynamics of the FF NiV epidemic model (45) when η = 1.00, 0.95, 0.95, 0.85, 0.80 and ϑ = 1.00, 0.97, 0.90, 0.85, 0.90: (a) virus concentration, (b) susceptible flying foxes, and (c) infected flying foxes.

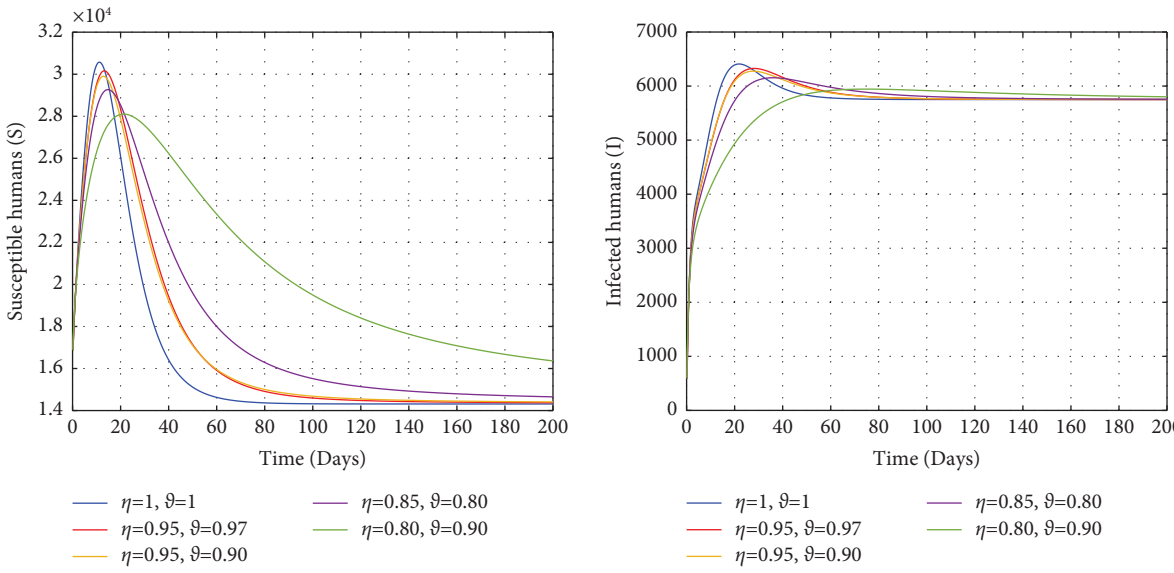

(a) (b)

Figure 12: Continued.

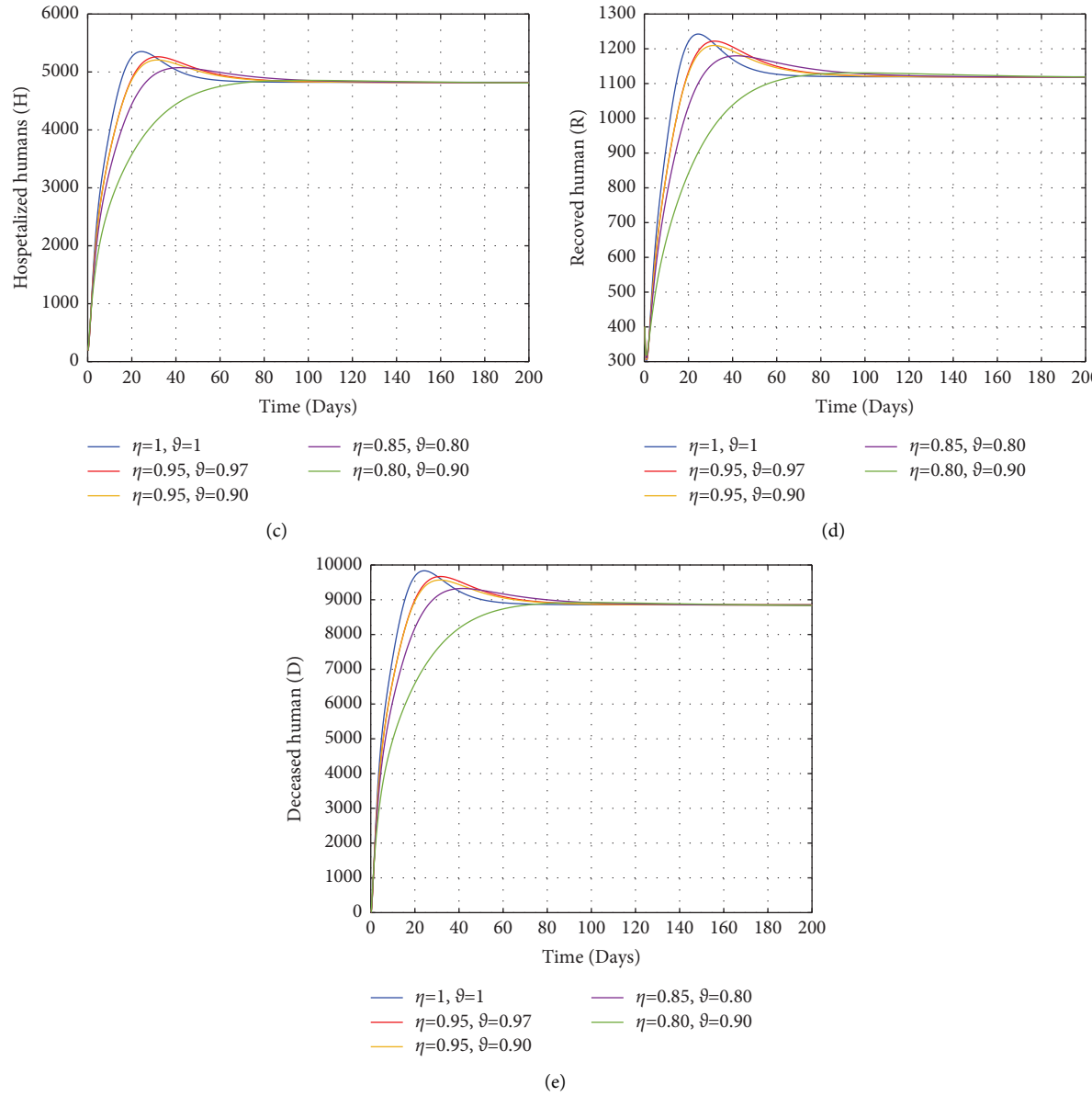

FIGURE 12: Case 17: simulation of the FF NiV epidemic model (45) when $\eta = 1.00, 0.95, 0.95, 0.85, 0.80$ and $\vartheta = 1.00, 0.97, 0.90, 0.85, 0.90$: (a) susceptible, (b) infected, (c) hospitalized, (d) recovered, and (e) deceased humans.

respective simulation by taking different combinations for the values of fractional order η and fractal order ϑ. The simulation results are illustrated in Figures 5–12. The detailed discussion and corresponding plots of each figure are given as follows.

Case 14. In this case, the NiV transmission model with FF operator (45) is simulated when $\eta = 1$ and by considering the fractal order $\vartheta \in (0, 1]$ with five values. The visual dynamics in this case are shown in Figures 5(a)–5(c) and 6(a)–6(e). Figure 5 shows subplots and Figures 5(a)–5(c) demonstrate the simulation results for the virus concentration, susceptible, and infected flying foxes. Figures 6(a)–6(e) analyze the dynamics of different human groups. It is noted that all population solution trajectories tend to converge towards the endemic equilibrium states.

Case 15. In the second scenario, we conduct simulations of the NiV epidemic model in FF case (45) with $\vartheta = 1$ while varying the fractional order η across five different values within the range of 0 and 1. The visual dynamics are depicted in plots 7 and 8 with subplots (a-c) and (a-e), respectively. The simulation of viruses' class, susceptible flying foxes, and infectious flying foxes is demonstrated

in Figures 7(a)–7(c), while Figures 8(a)–8(e) illustrate the behavior of susceptible, infected, hospitalized, recovered, and deceased human populations, respectively. Similar to a previous case, the model's solution tends to the steady state for all values of the fractional and fractal dimensions.

Case 16. In this case, we examine the dynamics of different population groups and concentrations of the virus while considering variations in both the fractional and fractal dimensions of the Caputo FF derivative. Both parameters, ϑ and η, are simultaneously varied in an equal manner (i.e., ϑ takes on values of 1.00, 0.95, 0.9, and 0.85, and η takes on values of 1.00, 0.95, 0.9, and 0.85) during the simulation of the NiV compartmental model in FF sense (45). The graphical analysis of the present case is illustrated in Figures 9(a)–9(c) and 10(a)–10(e). Outcomes in this section reveal that the solution curves reach a steady state over time.

Case 17. In the last case, we simulate the FF NiV epidemic model (45) where both the fractional and fractal parameters are changed simultaneously. However, in this case, both of these parameter values are considered unequally, i.e., $\eta = 1.00, 0.95, 0.95, 0.85, 0.80$ and $\vartheta = 1.00, 0.97, 0.90, 0.80, 0.90$. The simulation of this case is accomplished in Figures 11(a)–11(c) and 12(a)–12(e). Overall, from simulation in all cases, the solution treacheries are converged to the endemic steady state. However, in the last two cases, the convergence to an equilibrium point is obtained after a comparatively long period. In conclusion, the compartmental modeling approach utilizing the novel FF operators proves to be helpful for gaining a deeper understanding of the complex systems, including infectious diseases.

7. Conclusion

This study aims to illustrate the dynamics of NiV infection using a fractional and fractal-fractional modeling approach. NiV infection is one of the neglected infectious diseases that emerged in many Asian countries. We studied a new compartmental model with multiple transmission modes of Nipah virus infection. To the best of our knowledge, the study of NiV via the FF modeling approach could be the first attempt in the literature. The model was initially formulated using a system of eight nonlinear differential equations based on standard incidence rates. The food-born and human-to-human transmissions are considered in the model construction. A well-known Caputo operator in fractional only and fractal-fractional cases is used to construct the extended models. The existence and uniqueness of both extended models were provided, and possible equilibria of the problem were investigated based on the reproduction number. It is found that the model exhibits three equilibrium points, namely, infection-free, infected flying foxes free, and endemic steady state. The models were solved numerically using efficient iterative schemes, and an extensive simulation was performed for various values of only fractional order and then for both fractal and fractional dimensions simultaneously. The simulation results of the study showed that the FF NiV transmission model provides biologically more reliable results in all cases. Thus, we believe that such an advanced modeling approach can be confidently applied to address more complex real-life problems. In future, the proposed model can be extended using a fractional and fractal-fractional operator with nonsingular and nonlocal kernels.

Data Availability

The data used to support the findings of this study are included within the article.

Conflicts of Interest

The authors declare that they have no conflicts of interest.

Authors' Contributions

Shuo Li conceptualized and investigated the study, provided the software, and performed the formal analysis. Saif Ullah conceptualized the study, curated the data, provided the software, and wrote the original draft. Salman A. AlQahtani investigated the study, proposed the methodology, collected the resources, and supervised, visualized, and reviewed the study. Joshua Kiddy K. Asamoah provided the software and proposed the methodology, performed the formal analysis, validated and supervised the study, and reviewed and edited the manuscript.

Acknowledgments

This research was funded by the Research Supporting Project Number RSPD2023R585, King Saud University, Riyadh, Saudi Arabia. This work was also supported by the Undergraduate Education Teaching Research and Reform Project Foundation of Xinjiang Province (Grant no. XJGXZHJG-202213).

References

[1] World Health Organization, "Nipah virus," 2018, https://www.who.int/news-room/fact-sheets/detail/nipah-virus.

[2] World Health Organization, "Nipah virus (CDC)," 2020, https://www.cdc.gov/vhf/nipah/index.html.

[3] S. Kumar, R. Chauhan, S. Momani, and S. Hadid, "A study of fractional tb model due to mycobacterium tuberculosis bacteria," *Chaos, Solitons and Fractals*, vol. 153, Article ID 111452, 2021.

[4] X. Li and Y. Sun, "Application of rbf neural network optimal segmentation algorithm in credit rating," *Neural Computing & Applications*, vol. 33, no. 14, pp. 8227–8235, 2021.

[5] F. Arif, Z. Majeed, J. U. Rahman, N. Iqbal, and J. Kafle, "Mathematical modeling and numerical simulation for the outbreak of covid-19 involving loss of immunity and quarantined class," *Computational and Mathematical Methods in Medicine*, vol. 2022, Article ID 3816492, 21 pages, 2022.

[6] H. Li, R. Peng, and Z.-A. Wang, "On a diffusive susceptible-infected-susceptible epidemic model with mass action mechanism and birth-death effect: analysis, simulations, and comparison with other mechanisms," *SIAM Journal on Applied Mathematics*, vol. 78, no. 4, pp. 2129–2153, 2018.

[7] B. Sharma, S. Kumar, and C. Cattani, "Laminar convection of power-law fluids in differentially heated closed region: cfd analysis," in *Methods of Mathematical Modelling and Computation for Complex Systems*, pp. 45–63, Springer, Berlin, Germany, 2021.

[8] H.-Y. Jin and Z.-A. Wang, "Asymptotic dynamics of the one-dimensional attraction–repulsion keller–segel model," *Mathematical Methods in the Applied Sciences*, vol. 38, no. 3, pp. 444–457, 2015.

[9] A. Khan, R. Ikram, A. Din, U. W. Humphries, and A. Akgul, "Stochastic covid-19 seiq epidemic model with time-delay," *Results in Physics*, vol. 30, Article ID 104775, 2021.

[10] A. Khan and A. Din, "Stochastic analysis for measles transmission with lévy noise: a case study," *AIMS Mathematics*, vol. 8, no. 8, pp. 18696–18716, 2023.

[11] S. Ullah, M. A. Khan, M. Farooq, and T. Gul, "Modeling and analysis of tuberculosis (tb) in khyber pakhtunkhwa, Pakistan," *Mathematics and Computers in Simulation*, vol. 165, pp. 181–199, 2019.

[12] X. Xie, B. Xie, D. Xiong et al., "New theoretical ism-k2 bayesian network model for evaluating vaccination effectiveness," *Journal of Ambient Intelligence and Humanized Computing*, vol. 14, no. 9, pp. 12789–12805, 2022.

[13] X. Liu, S. Ullah, A. Alshehri, and M. Altanji, "Mathematical assessment of the dynamics of novel coronavirus infection with treatment: a fractional study," *Chaos, Solitons and Fractals*, vol. 153, Article ID 111534, 2021.

[14] S. Hussain, E. N. Madi, N. Iqbal, T. Botmart, Y. Karaca, and W. W. Mohammed, "Fractional dynamics of vector-borne infection with sexual transmission rate and vaccination," *Mathematics*, vol. 9, no. 23, p. 3118, 2021.

[15] M. A. Khan, S. Ullah, and S. Kumar, "A robust study on 2019-ncov outbreaks through non-singular derivative," *The European Physical Journal Plus*, vol. 136, no. 2, pp. 168–220, 2021.

[16] R. Alyusof, S. Alyusof, N. Iqbal, and S. K. Samura, "Novel evaluation of fuzzy fractional biological population model," *Journal of Function Spaces*, vol. 2022, Article ID 4355938, 9 pages, 2022.

[17] I. Podlubny, *Fractional Differential Equations: An Introduction to Fractional Derivatives, Fractional Differential Equations, to Methods of Their Solution and Some of Their Applications*, vol. 198, Elsevier, Amsterdam, Netherlands, 1998.

[18] M. Caputo and M. Fabrizio, "A new definition of fractional derivative without singular kernel," *Progress in Fractional Differentiation and Applications*, vol. 1, no. 2, pp. 1–13, 2015.

[19] A. Atangana and D. Baleanu, "New fractional derivatives with nonlocal and non-singular kernel: theory and application to heat transfer model," *Thermal Science*, vol. 20, no. 2, pp. 763–769, 2016.

[20] A. Atangana, "Fractal-fractional differentiation and integration: connecting fractal calculus and fractional calculus to predict complex system," *Chaos, Solitons and Fractals*, vol. 102, pp. 396–406, 2017.

[21] W. Wang and M. Khan, "Analysis and numerical simulation of fractional model of bank data with fractal-fractional Atangana-Baleanu derivative," *Journal of Computational and Applied Mathematics*, vol. 369, Article ID 112646, 2020.

[22] X.-P. Li, S. Ullah, H. Zahir, A. Alshehri, M. B. Riaz, and B. A. Alwan, "Modeling the dynamics of coronavirus with super-spreader class: a fractal-fractional approach," *Results in Physics*, vol. 34, Article ID 105179, 2022.

[23] S. Rezapour, J. K. K. Asamoah, A. Hussain et al., "A theoretical and numerical analysis of a fractal–fractional two-strain model of meningitis," *Results in Physics*, vol. 39, Article ID 105775, 2022.

[24] A. M. Alzubaidi, H. A. Othman, S. Ullah, N. Ahmad, and M. M. Alam, "Analysis of monkeypox viral infection with human to animal transmission via a fractional and fractal-fractional operators with power law kernel," *Mathematical Biosciences and Engineering*, vol. 20, no. 4, pp. 6666–6690, 2023.

[25] M. Biswas, "Model and control strategy of the deadly nipah virus (niv) infections in Bangladesh," *Research and Reviews in Biosciences*, vol. 6, no. 12, pp. 370–377, 2012.

[26] M. K. Mondal, M. Hanif, and M. H. A. Biswas, "A mathematical analysis for controlling the spread of nipah virus infection," *International Journal of Modelling and Simulation*, vol. 37, no. 3, pp. 185–197, 2017.

[27] C. Zúñiga-Aguilar, J. Gómez-Aguilar, H. Romero-Ugalde, H. Jahanshahi, and F. E. Alsaadi, "Fractal-fractional neuro-adaptive method for system identification," *Engineering with Computers*, vol. 1, 24 pages, 2021.

[28] D. Baleanu, P. Shekari, L. Torkzadeh, H. Ranjbar, A. Jajarmi, and K. Nouri, "Stability analysis and system properties of nipah virus transmission: a fractional calculus case study," *Chaos, Solitons & Fractals*, vol. 166, Article ID 112990, 2023.

[29] F. Evirgen, "Transmission of nipah virus dynamics under caputo fractional derivative," *Journal of Computational and Applied Mathematics*, vol. 418, Article ID 114654, 2023.

[30] K. A. Abro, A. Atangana, and J. Gómez-Aguilar, "Chaos control and characterization of brushless dc motor via integral and differential fractal-fractional techniques," *International Journal of Modelling and Simulation*, vol. 43, no. 4, pp. 416–425, 2022.

[31] K. A. Abro, A. Atangana, and J. Gomez-Aguilar, "Ferromagnetic chaos in thermal convection of fluid through fractal–fractional differentiations," *Journal of Thermal Analysis and Calorimetry*, vol. 147, no. 15, pp. 8461–8473, 2022.

[32] Z. M. Odibat and N. T. Shawagfeh, "Generalized taylor's formula," *Applied Mathematics and Computation*, vol. 186, no. 1, pp. 286–293, 2007.

[33] W. Lin, "Global existence theory and chaos control of fractional differential equations," *Journal of Mathematical Analysis and Applications*, vol. 332, no. 1, pp. 709–726, 2007.

[34] C. Li and F. Zeng, *Numerical Methods for Fractional Calculus*, Chapman and Hall/CRC, Boca Raton, FL, USA, 2015.

[35] D. Sinha and A. Sinha, "Mathematical model of zoonotic nipah virus in south-east asia region," *Acta Scientific Microbiology*, vol. 2, no. 9, pp. 82–89, 2019.

[36] A. D. Zewdie and S. Gakkhar, "A mathematical model for nipah virus infection," *Journal of Applied Mathematics*, vol. 2020, Article ID 6050834, 10 pages, 2020.

[37] A. D. Zewdie, S. Gakkhar, and S. K. Gupta, "Human–animal nipah virus transmission: model analysis and optimal control," *International Journal of Dynamics and Control*, vol. 11, no. 4, pp. 1974–1994, 2022.

[38] A. Atangana and S. Qureshi, "Modeling attractors of chaotic dynamical systems with fractal–fractional operators," *Chaos, Solitons and Fractals*, vol. 123, pp. 320–337, 2019.

[39] J. Ackora-Prah, B. Seidu, E. Okyere, and J. K. Asamoah, "Fractal-fractional caputo maize streak virus disease model," *Fractal and Fractional*, vol. 7, no. 2, p. 189, 2023.